Filipa Borralho Falcato

Licenciada em Bioquímica

Optimization and validation of methods for the determination of lipid composition in macroalgal matrices – characterization of undervalued red and brown macroalgae species

Dissertação para obtenção do Grau de Mestre em Química Bioorgânica

Orientador: Doutora Ana Maria Cardoso Lourenço Gomes Bispo, Investigadora, Instituto Português do Mar e da Atmosfera, I.P.

Elo de ligação: Doutora Paula de Sério Branco, Professora Auxiliar com Agregação, Faculdade de Ciências e Tecnologia da Universidade Nova de Lisboa

Júri:

Presidente: Professora Doutora Paula de Sério Branco

Arguente: Doutor Ricardo Jorge Guerra Calado

Vogal: Doutora Ana Maria Cardoso Lourenço Gomes Bispo

FACULDADE DE CIÊNCIAS E TECNOLOGIA
UNIVERSIDADE NOVA DE LISBOA

Dezembro, 2020

Filipa Borralho Falcato

Licenciada em Bioquímica

Optimization and validation of methods for the determination of lipid composition in macroalgal matrices – characterization of undervalued red and brown macroalgae species

Dissertação para obtenção do Grau de Mestre em Química Bioorgânica

Orientador: Doutora Ana Maria Cardoso Lourenço Gomes Bispo, Investigadora, Instituto Português do Mar e da Atmosfera, I.P.

Elo de ligação: Doutora Paula de Sério Branco, Professora Auxiliar com Agregação, Faculdade de Ciências e Tecnologia da Universidade Nova de Lisboa

Júri:

Presidente: Professora Doutora Paula de Sério Branco

Arguente: Doutor Ricardo Jorge Guerra Calado

Vogal: Doutora Ana Maria Cardoso Lourenço Gomes Bispo

FACULDADE DE CIÊNCIAS E TECNOLOGIA
UNIVERSIDADE NOVA DE LISBOA

Dezembro, 2020

Optimization and validation of methods for the determination of lipid composition in macroalgal matrices – characterization of undervalued red and brown macroalgae species

Acknowledgments

Firstly, my deepest thanks go to my supervisor, Dr. Ana Gomes Bispo, for tirelessly guiding me throughout this journey. For the patience and care; for the trust and encouragement; for the dedication and constant availability; for the countless pieces of advice and for perpetuating my growth throughout this year, I will always be grateful. It was an honour to learn from you and to have your support.

I would like to thank all the researchers and technicians of the Aquaculture, Upgrading and Bioprospecting Division (DivAV) of the Portuguese Institute for the Sea and the Atmosphere (IPMA), who somehow were part of my work. In particular, Dr. Narcisa Bandarra, Head of DivAV, for the encouragement and motivation, for always showing herself available and for all the unique opportunities I was given.

I would also like to thank to the project Algared+ "Rede Transfronteiriça para o Desenvolvimento de Produtos Inovadores com Microalgas", integrated in the programm "INTERREG V-A Espanha-Portugal (POCTEP)" for the grant and for funding this work.

I would also like to express my gratitude to Prof. Dr. Paula Branco for making this internship possible at IPMA and for all the availability shown throughout this year.

Finally, to my dear family and friends, thank you for being always present and for giving meaning to my journey. Thank you.

Abstract

Red and brown macroalgae are a natural source of bioactives, like polyphenols, carotenoids and polyunsaturated fatty acids (PUFA), with several industrial applications, including food and feed. Polar lipids (PL), such as glycolipids (GL), are an important fraction of macroalgae lipids standing out due to their antiviral, antioxidant, anti-inflammatory and antimicrobial activities. The present work aimed to optimize and validate an analytical protocol, based on an HPTLC (High Performance Thin Layer Chromatography) method, for the characterization of macroalgae lipid classes. Two extraction protocols were considered: Folch and Bligh and Dyer. The lipid composition of two red (*Asparagopsis armata* and *A. taxiformis*) and brown algae (*Treptacantha abies-marina* and *Cystoseira humilis*) were studied, along with the effect of drying conditions: sun and shade. Total lipid (TL) content ranged between 1.89-2.43% dw, in *C. humilis* (shade-dried, Folch) and *A. armata* (shade-dried, Bligh and Dyer), respectively. Both shade-dried *Asparagopsis* (Folch method) were the exception, showing higher contents: 3.15 and 3.20% dw (*A. armata* and *A. taxiformis*, respectively). The PL were globally the most abundant, especially in *A. taxiformis* (74.3 to 88.1% of TL, sun- and shade-dried, respectively). Among PL, monogalactosyldiacylglycerol (MGDG) was predominant, while triacylglycerols (TAG) and diacylglycerols (DAG) were predominant in non-polar lipids. The highest PUFA contents were observed in brown macroalgae, leveraged by high contents of arachidonic acid (ARA, 20:4 *n*-6), representing 14.0-17.4% of total fatty acids (FA) (sun-dried *Cystoseira* and shade-dried *Treptacantha*, respectively). Red algae, instead, contained mainly saturated fatty acids. The brown algae FA profile of PL highlighted phospholipids as the fraction with the highest PUFA amounts (40.7 and 43.5%, for *Cystoseira* and *Treptacantha*, respectively), where ARA accounted nearly 50% of total PUFA. Considering the ARA benefits including antitumoral activity and reduction of farmed fish larval stress, both *C. humilis* and *T. abies-marina* may be beneficial if incorporated in food and feed formulations.

Keywords: Polar lipids, HPTLC, FAME, *Cystoseira*, *Treptacantha*, *Asparagopsis*.

Resumo

As macroalgas vermelhas e castanhas são uma fonte natural de bioativos, como ácidos gordos polinsaturados (PUFA), com diversas aplicações industriais. Os lípidos polares (PL), nomeadamente os glicolípidos (GL), são uma importante fração, que se destaca pelas suas atividades antiviral, antioxidante, anti-inflamatória e antimicrobiana. O presente trabalho teve como objetivo otimizar e validar um protocolo analítico, baseado no método HPTLC (High Performance Thin Layer Chromatography), para a caracterização das classes de lípidos de macroalgas. Dois protocolos de extração foram considerados: Folch e Bligh e Dyer. Estudou-se a composição lipídica de duas algas vermelhas (*Asparagopsis armata* e *A. taxiformis*) e castanhas (*Treptacantha abies-marina e Cystoseira humilis*) e o efeito da secagem ao sol e à sombra. O teor de lípidos totais (TL) variou entre 1,89-2,43% dw: *C. humilis* (seca à sombra, Folch) e *A. armata* (seca à sombra, Bligh e Dyer), respetivamente. Ambas as *Asparagopsis* secas à sombra (Folch) foram a exceção: 3,15 e 3,20% dw (*A. armata* e *A. taxiformis*, respetivamente). Os PL foram os mais abundantes, especialmente em *A. taxiformis* (74,3 e 88,1% LT, seca ao sol e à sombra, respetivamente). Entre os PL, o monogalactosildiacilglicerol foi predominante, enquanto os triacilgliceróis e os diacilgliceróis predominaram nos lípidos apolares. Os maiores teores de PUFA foram observados nas macroalgas castanhas: elevados teores de ácido araquidónico (ARA, 20:4 *n*-6), representando 14,0-17,4% dos ácidos gordos totais (*Cystoseira* seca ao sol e *Treptacantha* seca à sombra, respetivamente). Nas algas vermelhas observaram-se, maioritariamente, ácidos gordos saturados. No perfil lipídico polar das algas castanhas, destacaram-se os fosfolípidos com maior conteúdo de PUFA (40,7 e 43,5%, para *Cystoseira* e *Treptacantha*, respetivamente), onde o ARA representou quase 50% do total de PUFA. Considerando os benefícios do ARA (atividade antitumoral e redução do stress de larvas de peixes cultivados), as macroalgas castanhas podem ser benéficas quando incorporadas em alimentos e rações.

Termos-chave: Lípidos polares, HPTLC, ácidos gordos, *Cystoseira*, *Treptacantha*, *Asparagopsis*.

Table of contents

List of figures

List of tables

List of abbreviations

ADC2	Automatic Development Chamber 2
ALA	α-Linoleic acid
ARA	Arachidonic acid
DAG	Diacylglycerol
DGDG	Digalactosyldiacylglycerol
DGTS	Diacylgyceryl-N-trimethylhomoserine
DHA	Docosahexaenoic acid
DW	Dry weight
EPA	Eicosapentaenoic acid
FA	Fatty acid
FAME	Fatty acid methyl ester
FFA	Free fatty acid
FID	Flame ionization detector
GC	Gas chromatography
GL	Glycolipid
HPTLC	High performance thin layer chromatography
IR	Infrared spectroscopy
LA	Linoleic acid
LoD	Limit of detection
LoQ	Limit of quantification
MAG	Monoacylglycerol
MGDG	Monogalcatosyldiacylglycerol
MS	Mass spectrometry
MUFA	Monounsaturated fatty acid

***n*-3**	Omega 3 fatty acid
***n*-6**	Omega 6 fatty acid
NL	Non-polar lipids
PC	Phosphatidylcholine
PE	Phosphatidylethanolamine
PL	Polar lipids
PLC	Preparative layer chromatography
PTLC	Preparative thin layer chromatography
PUFA	Polyunsaturated fatty acid
R_f	Retention factor
RSD	Residual standard deviation
SFA	Saturated fatty acid
SL	Sphingolipids
SQDG	Sulfoquinovosyldiacylglycerol
TAG	Triacylglycerol
TL	Total lipids
TLC	Thin layer chromatography

Thesis outline

The present work is divided into five main chapters:

Firstly, Chapter 1 (Introduction) focuses on the theoretical framework of this thesis, which entails important aspects concerning marine resources, namely, macroalgae, along with the role of lipids in this matrix, as well as HPTLC system principles and operation details. Procedures involved in analytical methods validation are also described.

Chapter 2 (Objectives) details the main objectives of this work.

The analytical methods used for lipids extraction, optimization, and validation, as well as lipid classes and profile determination and quantification, are explained in Chapter 3 (Materials and Methods).

In Chapter 4 (Results and Discussion) the results regarding the lipid classes analytical protocol optimization and validation, as well as the characterization of the lipid fraction are described. The discussion, based on the existing literature is also performed.

Finally, in Chapter 5 (Conclusions and future prospects) the key conclusions from the developed work are presented, together with future prospects considered important to advance the state of the art.

1. Introduction

1.1. Macroalgae: a global perspective and their importance as a source of bioactive compounds

The biodiversity in the seas is closely related to the wide diversity of marine origin compounds[1]. In fact, as life was born, developed, and became more complex in the seas, nearly half of the worldwide biodiversity is constituted by marine organisms, yet the vast majority of this territory remains unexplored. For this reason, oceans are considered a vast resource of new compounds and the largest remaining reservoir of bioactive natural molecules[1–3].

Algae are aquatic photosynthetic organisms that include in their composition a wide range of substances such as vitamins, minerals, pigments, polysaccharides, dietary fibres, polyphenols, amino acids, and lipids[4]. Among them, polysaccharides, polyphenols, carotenoids, and polyunsaturated fatty acids (PUFA) are some of the compounds with commercial importance for pharmaceutical, biomedical, and nutraceutical industries due to their antidiabetic, antioxidant, antibacterial, and antiviral activities[2,5–7]. The chemical composition of macroalgae, however, depends on the species, habitat, reproductive stage, salinity, temperature, light intensity, and environmental conditions[8].

Marine algae can be globally categorised into two main groups: microalgae and macroalgae (also known as seaweeds). Even though both can perform photosynthesis, they differ in a number of ways, like the size. While the first are microscopic and are often unicellular organisms, the second are macroscopic and more complex multicellular organisms. Furthermore, based on the presence of specific pigments like chlorophylls and carotenoids, macroalgae, can be classified into three main phyla: brown (Ochrophyta), red (Rhodophyta), and green algae (Chlorophyta)[9–11].

Historically, marine macroalgae have represented an important part of the human diet, especially in Asian countries like China, and Japan. Due to its unquestionable nutritional value, the consumption of macroalgae is no longer restricted to these populations and has increased in recent years[12]. Nowadays, in the literature, there can be found countless studies that highlight the beneficial effects of macroalgae extracts and their applications (Table 1.1).

Table 1.1 Macroalgae applications.

Application	Algae	Compound	Function	Ref.
Agriculture and horticulture industries	*Laminaria* spp., *Fucus* spp., *Ascophyllum nodosum*, *Sargassum* spp.	Polysaccharides, as laminaran	Stimulate natural plant defences responses	10,13
		Growth hormones, as auxins	Root-promoting activity	
		Betaine compounds	Resistance to biotic and abiotic stress	
Medicinal and pharmaceutical uses	*Chondrus crispus*, *Ecklonia cava*, *Asparagopsis taxiformis*	Phlorotannins, as dioxinodehydroeckol	Antiproliferative effect on human breast cancer cells	3,11,14,15
		Polysaccharides, as carrageenan	Block human papillomavirus types transmission	
		Aqueous and methanolic extracts	Treatment/prevention of oxidative stress-related diseases	
Biofuel	*Chlorococum* sp., *Spirogyra* sp.	Organic compounds (lipids, proteins, accumulation of polysaccharides as starch)	Fermentation for bioethanol production	16–19
Food additives	*Haematococcus* spp., *Laminaria* spp.	Carotenoids as astaxanthin	Food colouring	1,11
		Polysaccharides, as alginate kappa	Promotes flocculation and sedimentation of suspended solids in beer and wine	
Cosmetics	*Undaria pinnatifida*, *Gracilaria conferta*	Gametophyte extract (EPHEMER ™)	Antioxidant and anti-aging agent used in skin care products	20
		Gracilaria conferta powder	Humectant, nourishing and conditioning agent	

More recently, Pereira and Critchley[21] and *in silico* studies carried by Ahmed *et al.*[22] have associated macroalgae as a source of sulphated polysaccharides and alkaloids (as caulerpin), with potential antiviral applications against the novel SARS-CoV-2. According to Pereira and Critchley[21], these compounds have proved to inhibit the replication of enveloped viruses, namely, nidovirales. Furthermore, they can also be used in combination with other drugs. For instance, it was shown that the combination of the specific anti-influenza drug Zanamivir together with carrageenan increased survival of infected animals when in comparison with mono-therapies, due to their synergic action[23]. Beyond this, recently a Library of Marine Natural Products was screened, to identify potential SARS-CoV-2 protease inhibitors, including phlorotannins,

flavonoids, and pseudo peptides, reinforcing natural marine products utmost importance in the mitigation of disease[24]. Hence, it is worth mentioning the challenges that the marine biotechnology industry faces to identify new marine sources of bioproducts and develop novel screening technologies, based on a sustainable source of supply, which is crucial for the ecosystems health[1].

As a result of the growing interest concerning the multiple applications of macroalgae, the lipidic profile and the fatty acid (FA) analysis have been increasingly gaining importance[25]. When compared to other plant seeds, macroalgae contain low lipid contents, which often ranges between 1-5%[26]. Nonetheless, the lipids displayed contain important amounts of essential fatty acids, PUFA, and other functional lipid fractions[9,27]. The chemical composition of macroalgae, the lipid content, and, in particular, the FA profile, vary during the algal life cycle, as well as in different parts of the algal thallus. It also depends on the physiological state of the macroalgae, according to genetic status or taxonomic entity[27,28]. Different environmental conditions such as light intensity, salinity, depth, water temperature, nutrients, and pH can also have an impact on the lipid content and FA composition of these organisms[27,29–31]. For instance, it is known that the level of phosphorus and nitrogen concentration in seawater affect the FA profile of macroalgae[27,29,30,32] and that under favourable environmental conditions polar membrane lipids are generally the major lipid compounds present in macroalgae[33].

1.1.1. The red macroalgae *Asparagopsis armata* and *Asparagopsis taxiformis*

In some tropical and subtropical areas, red algae represent the primary component of the flora in terms of biomass and species diversity. It is believed that there are about 6000 species of red algae worldwide[27,34–36].

The dominance of red pigments, particularly of phycoerythrin and phycocyanin, which belong to the phycobilin group, mask the presence of other pigments, such as chlorophyll *a* and β-carotene, and are responsible for the colour of red macroalgae[9].

Red macroalgae, or Rhodophyta, differ from all other plants due to their polysaccharide composition, namely, agars and carrageenans, which find application as powerful gelling and stabilizing agents[34–36]. These macroalgae species have also been associated with high protein levels, averaging between 10 and 30% of their dry weight (dw). Brown macroalgae, in turn, seem to contain a lower protein content from 5 to 15% dw[26]. Furthermore, red algae contain higher amounts of carbohydrates and minerals, when compared to brown macroalgae[35].

Asparagopsis armata Harvey, 1855 (Figure 1.1) is distributed throughout Europe, namely in the Atlantic and in the Mediterranean basin. However, in Europe, these algae are often considered as an 'invasive species', meaning that they have been introduced and have interfered with the host ecosystem[37,38]. Both antioxidant and cytotoxic activities are reported for *A. armata*[37]. Besides, Haslin *et al.*[39] described *A. armata* as a source of compounds with anti-HIV activity, namely due to the presence of sulphated polysaccharides.

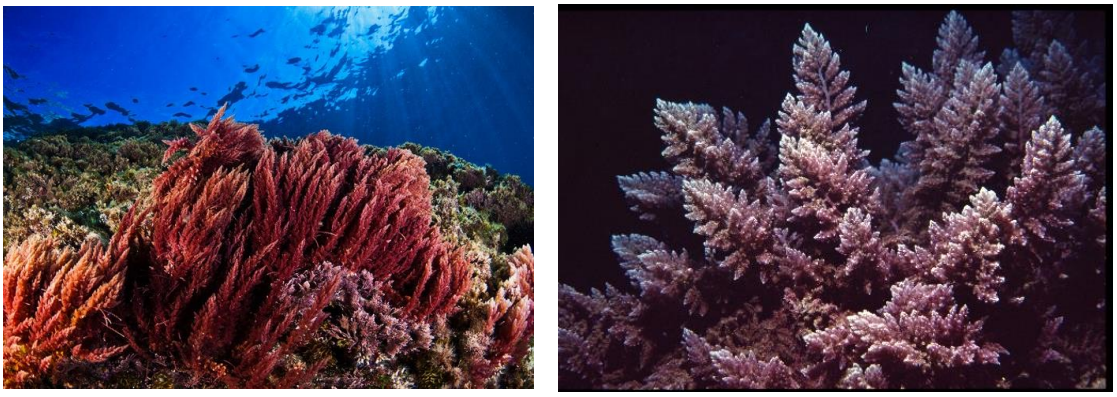

Figure 1.1 Macroalgae *Asparagopsis armata* (left): taken from https://www.feednavigator.com/Article/2019/07/09/Seaweed-slashes-methane-production-in-study-with-cows, 26/10/2020. Macroalgae *Asparagopsis taxiformis* (right): taken from https://www.marineforests.com/reports/732/, 26/10/2020.

Asparagopsis taxiformis (Delile) Trevisan, 1845 (Figure 1.1) is a red macroalgae species that belongs to the *Bonnemaisoniaceae* family. This medium-sized red macroalgal species has a broad global distribution, particularly in tropical and subtropical coasts of Pacific, Indo-Pacific, Atlantic, and Mediterranean regions[40]. Due to competition with *A. armata*, *A. taxiformis* became less common, in the Azores[41]. Due to their an antimethanogenic effect, both these macroalgae have been used for dairy cattle as a feed additive, as a way to reduced enteric methane emissions by over 50%[42].

1.1.2. The brown macroalgae *Cystoseira humilis* and *Treptacantha abies-marina*

Brown algae represent about 1836 different species in, approximately, 285 genera, occurring the vast majority of brown algal species in marine waters[27,43].

Due to its high fucoxanthin content, which is a xanthophyll pigment, these macroalgae show a brown colour. These algae also contain other pigments like chlorophyll *a* and *c* and β-carotene, that are masked by fucoxanthin[9].

Besides, brown macroalgae are rich in carbohydrates, namely alginate and cellulose which are structural components of the cell wall of these organisms. Other carbohydrates like laminarin and mannitol, are also present in brown algae where they play a storage role[9]. Fucoidan, known for

its biological activities such as anticoagulant and antithrombic properties, antiviral and antioxidant, has also been reported in brown macroalgae[9].

The genus *Cystoseira* is one of the most important brown algae genera found in the Mediterranean Sea and Atlantic Ocean ecosystems and, according to the criteria of the Water Framework Directive of the European Union, are considered as good indicators of high quality coastal waters[44,45].

Cystoseira humilis Schousboe ex Kützing, 1860 (Figure 1.2) belongs to the Sargassaceae family that can be found in the Mediterranean Sea, but also in the Azorean, Canaries, and Madeira archipelagos, particularly during spring between March and June when they are more abundant. Based on the available literature, *C. humilis* is referred to exhibit anticancer, antimicrobial, and antioxidative effects, making this species an interesting resource for the pharmaceutical, food, and cosmetic industries[46,47]. Vizetto-Duarte *et al.*[48] studied several species of *Cystoseira* sp., including *C. humilis*, and reported a balanced nutritional composition, suitable for human consumption. The authors found high contents of carbohydrates and a relatively high content of total lipids (TL) when compared to other species of macroalgae.

Treptacantha abies-marina (S.G.Gmelin) Kützing (Figure 1.2), previously known as *Cystoseira abies-marina,* is a medium-sized brown macroalgae abundant at the Azorean coast, but also at the Mediterranean Sea, Temperate Northern Atlantic, as well in the Canaries and Madeira archipelagos, especially between the period of March and June.

This edible macroalgae is considered as an interesting source of meroterpenoids, fucoxanthin, and phenolic compounds, as phlorotannins[44]. The research carried out by Barreto *et al.*[49] showed selective antiproliferative activity against HeLa tumour cells of *T. abies-marina* extracts. The same authors highlighted the potential of this macroalgae for application in the pharmaceutical, nutraceutical, food and/or cosmetics industry.

Figure 1.2 Macroalgae *Cystoseira humilis* (left): taken from https://marineforests.com/reports/407/, 26/10/2020. Macroalgae *Treptacantha abies-marina* (right): taken from https://seaexpert-azores.com/?page_id=2522, 26/10/2020.

1.2. Lipids and fatty acids in macroalgae

Lipids are a diverse group of compounds, which are mainly formed by hydrocarbon chains, the FA, but may also contain oxygen, phosphorus, nitrogen, and sulfur. These molecules can be found in their free form as free fatty acids (FFA) or esterified to different polar head groups, like glycerol[28]. The FA can be classified as saturated (SFA), if all carbon-to-carbon bounds are single, while those containing one double bound are designated as monounsaturated fatty acids (MUFA). When two or more double bounds can be found, these compounds are known as PUFA[9,30]. Among them, the essential fatty acids alpha-linolenic acid (ALA, 18:3 *n*-3) and linoleic acid (LA, 18:2 *n*-6) are of particular interest, since they cannot be produced by humans, as such, their intake from the diet is crucial to maintain their level in the organism[2,4,9,30,50,51]. Other FA like eicosapentaenoic acid (EPA, 20:5 *n*-3) and docosahexaenoic acid (DHA, 22:6 *n*-3), in turn, are not produced in adequate amounts. In fact, the FA profile is an important issue, once lipids biological activity, e.g. glycolipids (GL) are dependent on their FA content[52]. For example, EPA and DHA, are associated to a reduced risk of cardiovascular diseases, cancer, osteoporosis and diabetes[2,4,9,30,50]. Besides, PUFA regulate blood clotting and blood pressure, but also regulate inflammatory responses by producing inflammation mediators called eicosanoids[2].

Lipids are known to be involved in many vital biological functions in living beings. Even though they globally represent the source of energy for animals, plants, and microorganisms, they are also involved in a great variety of other processes[30]. The diversity observed in lipid structures is reflected in an enormous variety of functions of these molecules, due to the number of biochemical transformations, which occur during lipids biosynthesis[53].

Based on their polarity, lipids can be globally grouped as non-polar lipids (NL) and polar lipids (PL)[27,54,55]. The NL are, mainly, found in the form of triacylglycerols (TAG), which consist of a glycerol backbone esterified with three FA[28]. The TAG have storage and energy reservoir function, providing metabolic energy to cells[54]. Thus, while TAG act as a reservoir for FA, diacylglycerols (DAG) donates acyl groups for PL biosynthesis[53,54]. In turn, the polar counterparts are important structural components of cells[28]. The NL usually have a higher relative content of SFA and MUFA.

1.2.1. Polar lipids

The PL are referred to as the main source of lipids in some organisms, representing the core of macroalgae lipids[27]. Within the cell, they act as a selective but permeable barrier, being responsible for keeping membrane functions, to intermediate cell signalling pathways, and to respond to changes in the environment[28]. This is the case of GL, phospholipids, sphingolipids (SL), and betaine lipids that are key components of the membrane cells, and are involved in many

physiological functions, including photosynthesis for GL and phospholipids. For instance, SL have been associated with the inhibitory activity towards human leukemia cell growth, whereas betaine lipids are required for maintaining normal cell proliferation under phosphate-starved conditions[56,57].

1.2.1.1. Glycolipids

Macroalgae, as photosynthetic organisms, capture and use CO_2 as part of their photosynthetic process. When compared to terrestrial plants, macroalgae CO_2 fixation efficiency is between 10 and 50 times higher and it is estimated that about 40% of global photosynthesis is algal derived[58,59].

Located in the membrane of chloroplasts and thylakoids, GL are a less studied and the major class of PL, corresponding to the majority (80-90%) of lipids in these membranes, and more than half of all lipids of marine algae[7,52,55,60]. These compounds are defined by containing one or more monosaccharide residues bound by a glycosidic bound to a hydrophobic moiety[53,61]. The sugar moiety, the position of the glycerol linkage to the sugar, the length and location of the acyl chain, and the anomeric configuration of the sugar are directly related to GL bioactivities[55,62,63]. The monogalcatosyldiacylglycerol (MGDG), digalactosyldiacylglycerol (DGDG), and sulfoquinovosyldiacylglycerol (SQDG) are the three main types of glycoglycerolipids in macroalgae (Figure 1.3). The main difference among them relies on the composition of the glycosidic head group[27,54,55,62]. GL are rich in PUFA, such as ALA, LA, EPA, DHA, and arachidonic (ARA, 20:4 *n*-6) acids[52,55].

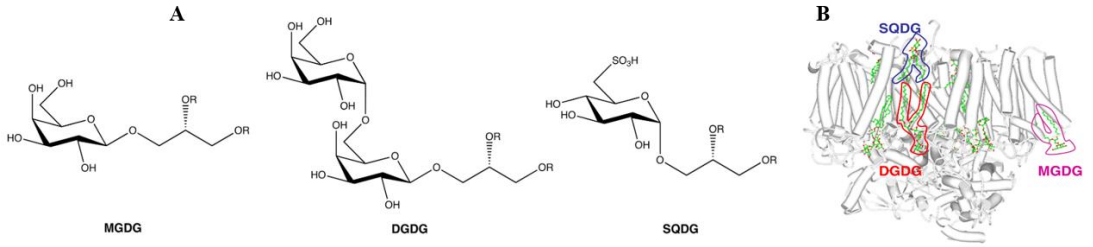

Figure 1.3 (A) Schematic representation of the general structure of the three main glycoglycerolipids from macroalgae – MGDG, DGDG, and SQDG (adapted from Plouguerné[62]). **(B)** Thylakoid lipids associated with the monomeric form of cyanobacterial photosystem II (adapted from Buodière[64]).

The MGDG and DGDG play key roles in the structural stabilization and function of membranes, as well as in the trafficking of lipids between subcellular compartments and photosynthesis, often being reported as the most abundant glycolipids[55,62,65]. According to White *et al.*[66], unlike MGDG and DGDG, evidence suggests that SQDG has no specific role in photosynthesis but can act as a substitute for phospholipid under conditions of phosphate limitation. Nonetheless, GL composition may vary on the availability of nutrients like carbon, nitrogen and phosphate. In fact, Wang *et al.*[67] found that cells do accumulate MGDG, DGDG, and SQDG when deprived of

nitrogen and phosphorus. In turn, Kumari *et al.*[68] observed that the absence of phosphate lead to the increase of SQDG and DGDG levels.

The most reported biological activities for GL from macroalgae are antibacterial, antitumoral, anti-inflammatory, and antiviral, which are related to the pharmacological potential of these compounds[55,62]. Regarding SQDG and its antiviral effect, literature suggests that the mechanism behind this bioactivity is related to the negatively charged sulfonate moiety, that may interact with the positive charges of viral proteins, similar to what happens with sulphated polysaccharides[69,70]. In this context, Souza *et al.*[71] suggested that SQDG antiviral effect may be upgraded in the presence of both MGDG and DGDG. These authors observed that SQDG activity was higher in the presence of MGDG and DGDG since a synergic effect was triggered. Likewise, palmitic acid also appears to have an active role in SQDG antiviral activity, since this FA prevents the entrance of HIV in cells and its dissemination[72,73]. SQDG isolated from *Spirulina palentesis* was also related to an antiviral activity towards simplex virus[70].

1.2.1.2. Other polar lipids

Phospholipids are characterized by having a phosphate group in the sn3 position of the glycerol backbone. Phosphatidylglycerol, phosphatidylethanolamine (PE), phosphatidylcholine (PC) are the main phospholipids present in macroalgae[28]. The specific head linked to the phosphate group determines the difference between these phospholipids: glycerol, ethanolamine (PE), choline (PC). For example, phosphatidylglycerol is essential for growth and the photosynthetic transport of electrons, and the development of chloroplasts[66]. In addition to their physiological role, phospholipids have been associated with various biological activities such as antibacterial, antiviral, and antitumoral, which have been contributing to the growing interest in this type of compounds. Indeed, it was found in both phospholipid fractions of *Sargassum marginatum* and *Porphyra yezoenzis* a high inhibitory effect of HL-60 cells (human leukaemia cell line) growth and a potent antitumor activity against Meth A fibrosarcoma, respectively[74].

The SL are also a part of the diverse group of membrane lipids found in marine organisms, namely in microalgae and some macroalgae species[75,76]. So far SL have only been reported in small amounts in red macroalgae[27]. These lipids contain a backbone of sphingoid bases, which is a set of aliphatic amino alcohols, including sphingosine. Structurally, SL comprise a diverse class, with a huge number of individual structures based on their variation in both SL backbone and head group[77,78]. The SL participate in cell-cell recognition, cell growth as second messengers, for instance in the brain. They have been also identified as biomarkers, in several diseases like cancer, diabetes, multiple sclerosis, and neuronal disorders, as most central nervous system disorders are linked with impaired lipid metabolism. Thus, changes in SL metabolism can result in the

rearrangement of the plasma membrane and the development of various neurological diseases, namely the progression of schizophrenia and metabolic syndromes[75,79].

Betaine lipids represent a class of both functional and structural lipids which also play an important role in macroalgae. The main known betaine lipid in macroalgae is diacylgyceryl-N-trimethylhomoserine (DGTS)[80,81]. It has been proposed that DGTS has the same function as the membrane associated phospholipid PC, due to their zwitterionic structure[81,82]. In fact, Meng *et al.*[83] observed in *Nannochloropsis oceanica* a negative correlation between the presence and abundance of DGTS and PC, as, after phosphorus starvation, PC amount almost vanished, whereas DGTS increased to be the highest polar lipid. Thus, since PC could be replaced with phosphorus-free DGTS to respond to phosphorus deprivation, changes in DGTS arise as a compensatory mechanism.

1.3. High Performance Thin Layer Chromatography (HPTLC)

In global terms, chromatography refers to a set of techniques used with the purpose to separate compounds, present in a complex mixture, through their distribution between two phases: the stationary and the mobile phase[84]. As such, it enables the separation and purification of the components of a mixture in order to allow a qualitative and quantitative analysis.

High performance thin layer chromatography (HPTLC) is based on the same principles as thin layer chromatography (TLC), however, it makes use of a more advanced system. The sophisticated instrumentation used in several steps, makes this technique an important asset for a standardized methodology of validated methods[85]. Indeed, the accurate sample application, the standardized and the reproducible chromatogram development, along with the software controlled evaluation are some of the most important advantages of this system. When compared with traditional TLC, other aspects are making HPTLC a more convenient system[86]:

- A shorter analysis time, as well as less cost per analysis, as several samples can be separated simultaneously.
- The equipment is relatively easy to operate.
- Lower amounts of solvents, as the required amount of mobile phase per sample is small (usually 35 mL).
- Higher separation efficiency.
- Efficient data acquisition and processing, through the possibility of scanning and proceed to spectrum analysis.
- Use of different universal and selective detection methods.

Due to its uniformity, precision, and accuracy of results, HPTLC is known for its versatility, since it can handle several samples simultaneously[84]. This approach is suitable for both qualitative and

quantitative analysis of a wide range of compounds, such as various types of medicines, herbal and botanical dietary supplements and nutraceuticals, with a wide range of applications in cosmetics, food and pharmaceutical industries, quality control, forensics and clinical applications (in metabolism studies for drug screening)[85–88].

In order to improve detection selectivity and sensitivity, the coupling of two or more analytical techniques to HPTLC is a strategy that can be adopted. Thereby, coupling the HPTLC with other analytical techniques, such as mass spectrometry (HPTLC-MS[89,90]) or infrared spectroscopy (HPTLC-IR), brings an added level of information to HPTLC[91].

1.3.1. The principle

The separation of the different compounds is based on the interaction of the analytes with the stationary (where the sample is loaded) and the mobile phases (in which the sample is carried, through capillary action)[84,92]. The upward travelling rate, known as the retention factor (R_f), depends on the polarity of the compounds in analysis, as well as on the stationary and mobile phases[92]. In other words, the migration rate depends on the compounds relative affinity towards stationary and mobile phases. For those components having less affinity towards the stationary phase (and more with the mobile phase), the migration will be higher, when compared to those components with more affinity towards the stationary phase. This phenomenon results in the formation of different bands or zones according to each component migration[84].

1.3.2. The procedures

The HPTLC system includes a set of semi-automated equipments in which the sample application, the development, the derivatization, and the detection are performed. Additionally, each of these equipments and the respective parameters are controlled using a common software[93].

1.3.2.1. Sample application

The sample application is the most critical step to obtain a good resolution of the chromatographic separation and to ensure results quality at the end of the process[85,87]. A precise sample application can be accomplished using, for example, the Linomat 5 (CAMAG) (Figure 1.4), through a semi-automatic process, in which only the syringe is handled (to fill, insert into the equipment and rinse).

Figure 1.4 Scheme of the instrument Linomat 5 (adapted from CAMAG[93]).

With a system like Linomat 5 samples are applied by spraying onto HPTLC plates in the form of bands. The sample is, preferably, sprayed with an inert gas, commonly, nitrogen, however compressed air, can also be used[93].

The sample is loaded in a dosage syringe of 100 µL or 500 µL and TLC plates used have dimensions up to 200 x 200 mm. Before samples application, multiple parameters like sample volume, band length and the distance between bands must be adjusted[93].

1.3.2.2. Development

In the development step, the plate is immersed in the mobile phase, and separation is achieved as previously explained. The use of the Automatic Development Chamber (ADC2, CAMAG) (Figure 1.5) enhances the reproducibility of the results, since the development process is automatically monitored, and takes place under controlled conditions, namely in terms of relative humidity.

Figure 1.5 Scheme of the instrument ADC2 (adapted from CAMAG[94]).

The plate precondition parameters, the solvent migration distance, and the drying conditions are set in the controlling software prior to analysis. The pre-condition step ensures that the chamber

is properly saturated with a vapor phase of the solvent mix, preventing the front solvent evaporation, which otherwise would increase R_f values[94].

1.3.2.3. Derivatization

In the derivatization process, specific reagents are used to enable the detection of substances that otherwise would not be detectable. This is undertaken through a chemical reaction that converts the non-absorbing substances into detectable derivatives, or derivatives with improved detectability[88]. In HPTLC and TLC protocols, it can be performed either by immersion or by spraying. However, it is noteworthy, that derivatization by immersion is the best option in terms of bands definition and reproducibility. Derivatization by immersion can be achieved with, for instance, the Chromatogram Immersion Device 3 (CAMAG), used for automatic dipping. Through the immersion of the plate with a controlled vertical speed into the derivatization reagents, derivatization conditions can be standardized and "tide marks", which can interfere with the densitometric evaluation, can be avoided[95].

1.3.2.4. Detection

The detection under non-destructive systems, using visible or UV light are usually the first choice. The offline operation of HPTLC systems means that multiple methods can be used for compounds detection and identification[88].

The detection carried out with the TLC Scanner 4 (CAMAG), Figure 1.6, is based on densitometric measurements.

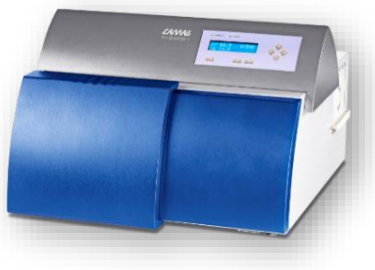

Figure 1.6 Scheme of the instrument TLC Scanner 4 (adapted from CAMAG [96]).

Through densitometry, it is possible to quantify the amount of each analyte by measuring the optical density of the separated spots directly on the plate. The analytes concentration may be determined, for example, by comparison with a standard curve, using standards with known concentrations that are chromatographed simultaneously with the samples, under the same conditions[97]. For this equipment, both absorption or fluorescence modes are possible[96]. After

densitometric measurements, data can be further processed by CAMAG visionCATS/winCATS software.

1.4. Validation of analytical methods

The validation of analytical methods is a valuable tool to ensure that a specific method can produce accurate and precise results[98,99]. This process allows guaranteeing, that the selected method is suitable for the analysis of an analyte in a certain matrix[100]. Therefore, the validation of analytical methods represents a tool to establish the necessary control to obtain reliable analytical data.

Method validation should be carried out alongside method development, where the viability of the study must be considered. Accordingly, method validation is the last step for the success of the whole method development process. The definition of the analytical aim before method selection, development, and optimization is decisive. For this reason, at the initial stage, a careful literature review must be carried out, since available information will be useful to understand the further study. In order to structure, control and document the validation process, the validation protocol is a key instrument[88].

1.4.1. Specificity

A method is considered acceptable, in terms of specificity, if no interference between each analyte is detected, in this case, each lipid class, represented in the form of bands[101]. The ability of an analytical method to unequivocally assess the analyte in the presence of other components evaluates a method specificity[102]. Thus, for a method to be considered specific, the following condition $R_s > 1.5$, between two consecutive peaks, has to be verified[103]. The determination of HPTLC peaks resolution should be carried by the following equation:

$$R_s = 2 \times \frac{Max\ R_f\,(2) - Max\ R_f\,(1)}{\left(End\ R_f\,(2) - Max\ R_f\,(2)\right) + \left(End\ R_f\,(1) - Max\ R_f\,(1)\right)} \qquad \text{(Eq. 1.1)}$$

Where the $Max\ R_f\,(1)$ and $Max\ R_f\,(2)$ correspond to the peak apex (maximum retention factor) of two consecutive peaks and $End\ R_f$ corresponds to the peak end.

1.4.2. Calibration curve and working range

Throughout the estimation of the mathematical expression of the calibration curve, it is possible to correlate the system measurements with a known concentration or amount of substance[101]. Quantification requires that the dependence between the measured response and the analyte concentration is known. To estimate the mathematical expression of the calibration curve some important steps are needed: the preparation of pure standard solutions with known concentration;

the analysis of standards solutions in the same analytical equipment and conditions as samples and the determination of the calibration curve. The aforementioned calibration curve will be then used to determine analyte concentration by interpolation[101].

The equation of the calibration curve is given by:

$$y = a + bx \quad \text{(Eq. 1.2)}$$

In which a corresponds to the interception of y axis and b to the slope.

One of the parameters which can be used for the analytical calibration evaluation is the correlation coefficient (ρ):

$$\rho = \frac{\sum_{i=1}^{N}\{(x_i - \bar{x}) \times (y_i - \bar{y})\}}{\sqrt{\left[\sum_{i=1}^{N}(x_i - \bar{x})^2 \times \left\{\sum_{i=1}^{N}(y_i - \bar{y})^2\right\}\right]}} \quad \text{(Eq. 1.3)}$$

This parameter covers a range of values between -1 (negative correlation which corresponds to a negative slope) and +1 (positive correlation which corresponds to a positive slope). According to Guia Relacre[101], values above 0.995 should be obtained for the correlation coefficient of calibration curves. Despite this parameter indicating the adjustment of the results, it is not conclusive relatively to the method linearity[101].

The working range of an analytical method corresponds to the range of concentrations in which the analytical procedure is precise and accurate.

The calibration curve can be estimated following a linear model (as recommended in ISO 8466-1) or a second-degree polynomial fit (as recommended in ISO 8466-2)[101]. The working range is determined using the homogeneity of variances test for the lowest (S^2_1) and highest (S^2_{10}) concentration standards, for $i = 1$ and $i = 10$[101]:

$$S_i^2 = \frac{\sum_{j=1}^{10}(y_{i,j} - \bar{y_i})}{n_i - 1} \quad \text{(Eq. 1.4)}$$

$$\bar{y_i} = \frac{\sum_{j=1}^{10} Y_{i,j}}{n_i} \quad \text{(Eq. 1.5)}$$

Where i corresponds to the standard number, between 1 and 10, j corresponds to the number of repetitions for each standard, y_i to the equipment signal and $\bar{y_i}$ corresponds to the mean value of the signal.

In order to evaluate if there are significant differences in variances, for working range limits, the PG test value is determined according to[101]:

$$PG = \frac{S_{10}^2}{S_1^2} \quad \text{(Eq. 1.6)}$$

For $S_{10}^2 > S_1^2$ and

$$PG = \frac{S_1^2}{S_{10}^2} \quad \text{(Eq. 1.7)}$$

For $S_1^2 > S_{10}^2$.

The PG test value is then compared with the Snedecor/Ficher F distribution table value, for n-1 degrees of freedom. Whenever PG ≤ F is verified, differences in variances are not significant, meaning that the working range is adjusted. In turn, if $PG >$ F, variances have significant differences and the working range should be reduced until the first condition is fulfilled (PG ≤ F)[101].

1.4.3. Analytical limits

The concept of the limit of detection (LoD) and the limit of quantification (LoQ) is of great importance once it indicates the minimum analytical thresholds at which is possible to detect and quantify the analyte with certain precision and accuracy[101,104].

Both these parameters rely on the measured variable, thus dilutions on the samples must be considered. LoD and LoQ depend on several aspects such as contaminations, the sample itself, the equipment, and the operator. Whenever changes in the routine method take place, it is necessary to re-evaluate the analytical limits[101].

1.4.3.1. Limit of Detection

The LoD is defined by the minimum concentration in which it is possible to detect an analyte, corresponding to the lowest analyte amount that is possible to detect in a sample. Although detected, the analyte is not necessarily quantified, as the quantification associated with this value entails significant errors[101,104,105].

In analytical methods evolving blank replicates or trace standards, LoD is expressed by[101]:

$$LoD = x_0 + 3.3s_0 \quad \text{(Eq. 1.8)}$$

In which, $x_0$corresponds to the arithmetic mean of the measured content of a series of blanks or trace patterns (between 10-20 trials), independently prepared, s_0 corresponds to the x_0 standard deviation and 3.3 represent K value which is a numerical factor with a statistical confidence of 99.7%.

1.4.3.2. Limit of Quantification

The lowest measured concentration in which it is possible to make a quantitative detection of the studied analyte corresponds to the LoQ. In practice, this value often corresponds to the lowest concentration standard (excluding the blank) used to determine the calibration curve[101].

LoQ is generally determined as follows[104]:

$$LoQ = x_0 + 10s_0 \quad \text{(Eq. 1.9)}$$

Where x_0, represents, as mentioned above, the arithmetic mean of the measured content of a series of blanks or trace patterns (between 10-20 trials), independently prepared, s_0 corresponds to the x_0 standard deviation. The K value for the LoQ is 10.

1.4.4. Precision

Precision refers to the degree of agreement between results of independent measurements under conditions of repeatability or reproducibility, therefore both these concepts allow the evaluation of precision dispersion. Precision provides an indication of random error. A method precision is expressed through the standard deviation also known as the coefficient of variation[84,101,106].

1.4.4.1. Repeatability

The repeatability is determined through a test method, carried out for the same sample standard under similar conditions, in a short period. This means, that the measurement procedure is the same, as well as, the laboratory, the operator, and the equipment. For the determination of repeatability, it is required a minimum of 10 tests ($n \geq 10$)[101].

The limit of repeatability (r) is the maximum admissible value for the absolute difference between two tests, in repeatability conditions, determined for a level of confidence of 95%:

$$r = 2.8 \times S_{ri} \quad \text{(Eq. 1.10)}$$

Where, S_{ri}, corresponds to the standard deviation of the repeatability associated with the considered results[101,106].

The repeatability coefficient of variation, for each level of concentration, is given by[101]:

$$\%RSD = \frac{S_{ri}}{\bar{x}} \times 100 \quad \text{(Eq. 1.11)}$$

Where %RSD is numerically identical to repeatability standard deviation divided by the mean of the considered values, $\bar{x}$.

1.4.4.2. Reproducibility

The reproducibility of a method refers to the method precision carried under different experimental conditions, namely a different operator, laboratory, equipment and repeated over long intervals of time. Although, the same procedure must be followed.

The reproducibility limit (R) is given by the value under the absolute difference between two test results, obtained in the condition mentioned above, with a specific probability (95%), which is determined by[101]:

$$R = 2.8 \times S_{Ri} \qquad \text{(Eq. 1.12)}$$

Where, S_{ri} corresponds to the standard deviation of the reproducibility associated with the considered results[101].

The coefficient of variation of reproducibility is given by[101]:

$$CV_R = \frac{S_{Ri}}{\bar{x}} \times 100 \qquad \text{(Eq. 1.13)}$$

Where CV_R is numerically identical to reproducibility standard deviation divided by the mean of the considered values, $\bar{x}$.

1.4.4.3. Intermediate precision

The estimated precision for the same sample or standard, using the same method, in the same or different laboratories, establishing which conditions should be changed corresponds to the intermediate precision. Thus, the intermediate precision study allows to evaluate the interference of changing, for instance, the operator, the equipment, or the time interval in the results; for this reason, intermediate precision is the most representative of the variability of the results in a laboratory[101,106]:

The value of intermediate precision is determined with the following expression:

$$Si_{precision} = \sqrt{\frac{1}{t(n-1)} \sum_{j=1}^{t} \sum_{k=1}^{n} (y_{jk} - \bar{y_j})^2} \qquad \text{(Eq. 1.14)}$$

This equation reflects the dispersion results, in which, $Si_{precision}$ corresponds to the standard deviation of intermediate precision; t corresponds to the number of samples; n corresponds to the number of tests for each sample; j corresponds to the number of the sample ($1 \leq j \leq t$); k corresponds to the obtained result for the sample j; y_{jk} corresponds to the individual result of the sample j; $\bar{y_j}$ represents the arithmetic mean of the results for the sample j[101,106].

2. Objectives

Today's consumers have a strong awareness of the relationship between diet and health, which has led to an increased demand for foods with benefits for human health. Among them, macroalgae arise as a source of unique bioactive compounds, including their lipids. Even though macroalgae often present a low amount of lipids, their composition, rich in PL like GL, is recognized by their antibacterial, antitumoral, anti-inflammatory, and antiviral activities. Furthermore, these lipids typically contain important amounts of *n*-3 PUFA, like EPA and DHA. As a result, the presence of these beneficial compounds associated with the great diversity of these marine organisms, where many species lack information regarding their composition, substantiates the importance of this study, having the characterization of PL fraction and GL as its main focus.

In global terms, the present work aimed to address three main objectives:

1. **Selection of the best analytical method for lipid extraction from macroalgal matrices**

A thick cell wall and the presence of different pigments are some of the major interferences that difficult the assessment of macroalgae lipid composition. The methods commonly used are not as efficient as they should extract lipids from this matrix, thereby, it becomes imperative to choose the best alternative.

2. **Optimization and validation of a method for lipid classes determination using HPTLC**

The HPTLC is a powerful chromatographic tool to separate analytes in complex mixtures, as it happens with macroalgae lipid extracts. The optimization and validation of an analytical procedure using this system allows to set the best chromatographic conditions for a robust and rigorous determination of macroalgae main lipid classes. The optimization was carried out considering the best options to improve the separation and quantification of PL classes, in particular, GL.

3. **Characterization of the lipid fraction of four macroalgae species**

Finally, this work aimed to carry out the characterization of the lipid fraction of four undervalued macroalgae species, in terms of their TL content, lipid classes composition, FA profile, and FA composition of PL classes. The red algae *A. armata* and *A. taxiformis* and the brown algae *T. abies-marina* and *C. humilis* were the selected species. The experimental design followed for the characterization of the macroalgae lipid fraction is summarized in Figure 2.1.

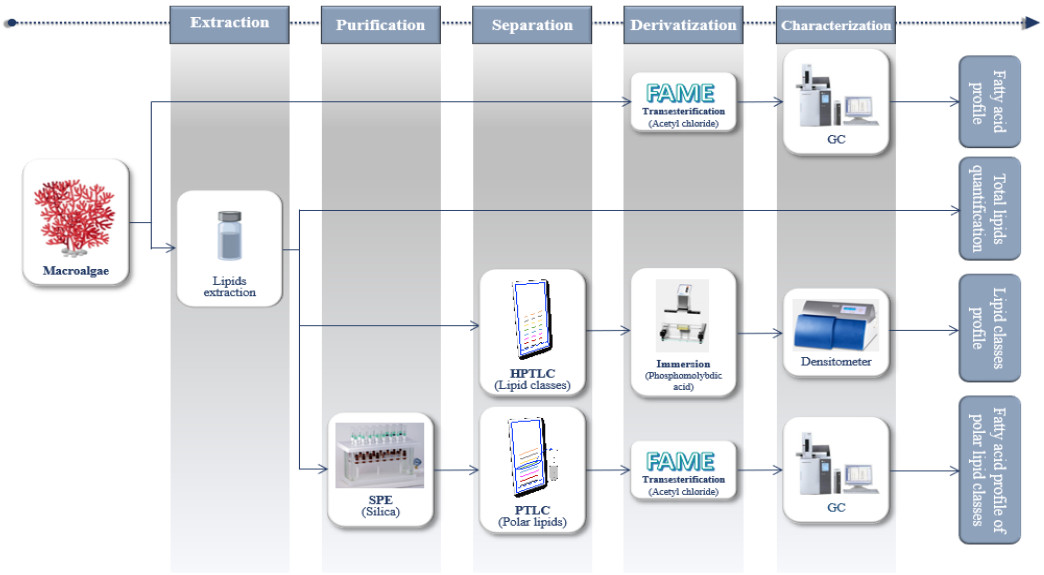

Figure 2.1 Experimental design followed for the characterization of the macroalgae lipid fraction.

3. Materials and Methods

3.1. Reagents and Standards

Chloroform (≥ 99.0% (v/v), p.a.), methanol (≥ 99.0% (v/v), p.a.), anhydrous sodium sulphate (≥ 99.0% (w/w), p.a.), molybdenum(VI) oxide (≥ 99.5%, p.a.) and sodium chloride (≥ 99.5%, p.a.) were acquired from Carl Roth (Germany), methyl acetate (99.0%, p.a.) was purchased from Fluka (U.S.A.), isohexane (≥ 98.0%, p.a.), acetyl chloride (≥ 98.0%, p.a.), acetic acid (99.8% (v/v), p.a.), acetone (≥ 99.8%, p.a.), absolute ethanol (100.0% (v/v) p.a.), isopropanol (p.a.), *ortho*-phosphoric acid (85.0%), hydrated phosphomolybdic acid (p.a.) and diethyl ether (> 99.7% (v/v), p.a.) were from Merck (Germany), n-heptane (> 99.0% (v/v), p.a.) and hydrochloric acid (37.0%, p.a.) was from Riedel-de Haen (Germany), sulphuric acid (95.0-97.0%, (v/v)), magnesium chloride ($MgCl_2$) (99.0% (w/w)), dichlorofluorescein, copper (II) acetate monohydrate and orcinol monohydrate (≥ 99.0%, HPLC) were from Sigma-Aldrich (U.S.A.), potassium chloride (99.0% (w/w)) was from CalbioChem and acetonitrile (≥ 99.9%, p.a.) was from Scharlau (Spain). Water was obtained from a Millipore (U.S.A.) Milli-Q water purification system.

The pure standards used for the lipid classes identification of PC (L-α-phosphatidylcholine, P3556), PE (L-α-phosphatidylethanolamine, P6386), SL (galactocerebroside from bovine brain, C4905), 1,2-diacylglycerol (1,2-DAG) (1,2-dioleoyl-rac-glycerol, D8394), TAG (glycerol triolein, T7140), FFA (oleic acid, O1008) were purchased from Sigma-Aldrich (U.S.A.). During the optimization process, a standard mixture containing monoolein (monoacylglycerol, MAG), 1,2-dioleoyl-rac-glycerol (1,2-DAG), 1,3-diolein (1,3-DAG) and glycerol triolein (TAG) supplied from Supelco (U.S.A.) was also used. The pure standards of SQDG (840525P), DGDG (840524P) and MGDG (840523P) were purchased from Avanti Polar Lipids (U.S.A.), PUFA No.3 (47085-U) and heneicosanoic acid (21:0) (H5149) were bought from Supelco (U.S.A.).

3.2. Materials and equipment

- Analytical Balance Explorer EX224M (Ohaus, U.S.A.).
- Centrifuge (Sigma, 2K 15, Germany).
- Chromatogram immersion device 3 (CAMAG, Switzerland).
- Column DB-WAX 30 m, 0.25 mm, 0.25 μm (Agilent Technologies, U.S.A.).
- Dosage syringe 100 μL for Linomat 5 (CAMAG, Switzerland).
- Glass-cutter.
- Grindomix GM 200 (Retsh, Germany).
- Heating oven (Memmert, Germany).

- Linomat 5 (CAMAG, Switzerland).
- Polytron PT 10-35 GT-D (Kinematica, Switzerland).
- Rotatory evaporator (Buchi 461, Switzerland) and vacuum pump (Buchi V700, Switzerland).
- Scion 456-GC gas chromatograph (Bruker, U.S.A.).
- Silica gel 60 F_{254} 20x20 preparative layer chromatography (PLC) plates, 0.25 mm thickness (Merck, Germany).
- Silica gel 60 F_{254} HPTLC glass plates, size 20 x 10 cm, 0.5 mm thickness (Merck, Germany).
- SPE 500 mg (Isolute).
- Thermostatic bath (Buchi 461, Switzerland).
- TLC glass atomizer.
- TLC Scanner 4 (CAMAG, Switzerland).
- Twin through chamber for 20 x 10 cm plates (CAMAG, Switzerland).
- Common laboratory apparatus.

3.3. Solutions

3.3.1. Standards stock and working solutions

Pure standards stock solutions were prepared with chloroform as described in Table 3.1.

Table 3.1 Conditions in which pure standards were prepared.

Standard	Mass (mg)	Final volume (mL)	Concentration (mg/mL)
PC	10	10	1
PE	1	1	1
SQDG	5	1	1
DGDG	5	5	1
SL	10	25	0.4
MGDG	5	5	1
1,2-DAG	1	1	1
FFA	10	1	10
TAG	10	1	10

Then, the working solution (pool) at 1 mg/mL was prepared, combining the individual standards PC, PE, SQDG, DGDG, SL, MGDG, 1,2-DAG, FFA, and TAG. This solution was used as a reference to confirm the lipid classes retention factor (R_f).

3.3.2. Cupric acetate solution (lipid classes quantification)

Thirty grams of copper (II) acetate monohydrate were dissolved in 80 mL of *ortho*-phosphoric acid (85 %). This solution was added with 920 mL of H_2O Milli-Q. The cupric acetate solution was stored protected from light.

3.3.3. Phosphomolybdic acid (lipid classes quantification)

Both 5 and 10% phosphomolybdic acid solutions were prepared. Five or 10 g of phosphomolybdic acid were dissolved in 100 mL of absolute ethanol, to prepare a solution at a final concentration of 5 or 10%, respectively. Both solutions were kept under refrigeration and protected from light.

3.3.4. Orcinol-sulphuric acid solution (GL confirmation)

Orcinol (125 mg) was dissolved in 42 mL of H_2O Milli-Q and, under agitation, 25 mL of sulfuric acid were slowly added. Then 67.5 mL of ethanol absolute was added. This solution is stable for a week. During that period, it was kept under refrigeration and protected from light.

3.3.5. Dittmer & Lester solution (phospholipids confirmation)

Solution I

Eight grams of MoO_3 were dissolved, in 200 mL of sulphuric acid 70%. This solution was boiled under gentle stirring until complete dissolution. The solution was then cooled to room temperature.

Solution II

After the addition of 0.4 g of molybdenum powder to 100 mL of solution I, the mixture was boiled for 1 h and cooled to room temperature.

Solution III

To a 100 mL of solution I were added 100 mL of solution II (1:1 v/v).

Derivatization spray

Fifty millilitres of solution III were added to 100 mL of H_2O Milli-Q and 37.5 mL of acetic acid (1:2:0.75 v/v/v). This solution was stored protected from light and was stable for 6 months.

3.3.6. Dichlorofluorescein solution

The dichlorofluorescein 0.2% (w/v) was prepared by dissolving 200 mg in 100 mL of absolute ethanol. This solution was stored protected from light and under refrigeration.

3.4. Macroalgae samples

The four species of macroalgae: *A. armata* and *A. taxiformis* (Rhodophyta), and *T. abies-marina* and *C. humilis* (Ochrophyta) that were selected and used in this study are shown in Figure 3.1. Macroalgae samples, supplied by the company seaExpert, were harvested between April 2019 and May 2019, in Faial island in the Azores (Portugal). For each species, two different drying conditions were considered: sun and shade-dried. Sun-dried samples were dried in a greenhouse (3-5 days), in which temperature varied from 28 to 35 ºC and 18 to 22 ºC, during day and night, respectively. In turn, shade-dried samples were dried in a solar dryer with ventilation, at 35 - 40 ºC.

After arriving at the Portuguese Institute for Sea and Atmosphere (IPMA) laboratory, in Lisbon, macroalgae were freeze dried and homogenised to powder with a Grindomix GM 200 (Retsh, Germany). Macroalgae were then deep frozen and stored at -80 ºC until they were analysed.

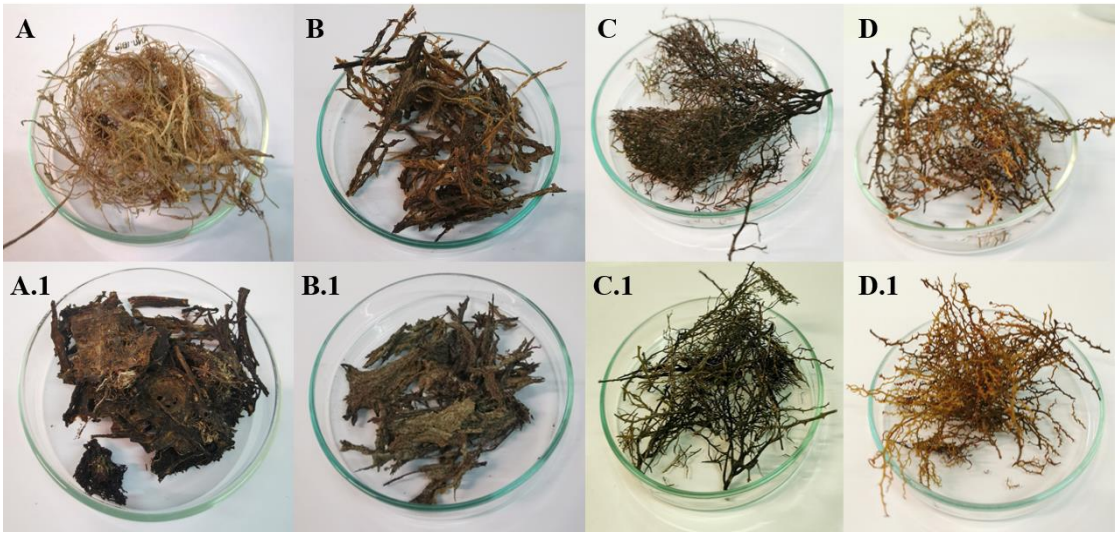

Figure 3.1 Macroalgae species in this study: sun-dried *A. armata* (**A**), shade-dried *A. armata* (**A.1**), sun-dried *A. taxiformis* (**B**), shade-dried *A. taxiformis* (**B.1**), sun-dried *C. humilis* (**C**), shade-dried *C. humilis* (**C.1**), sun-dried *T. abies-marina* (**D**) and shade-dried *T. abies-marina* (**D.1**).

3.5. Total lipids content

The selection of the best analytical procedure for TL extraction was based on the two most widely used methodologies: Bligh and Dyer[107] and Folch[108], in order to obtain the maximum extraction of lipids, with the least possible interference. For each of these analytical protocols, the extracts obtained were further analysed and lipid classes were identified. This approach allowed to evaluate the extraction performance, in terms of the lipid classes that were extracted, as well as in the identified lipid classes. Analyses were performed in triplicate.

Bligh and Dyer method

One gram (P_a) of previously homogenised algal biomass was weighted to a test tube, added with 5 mL of extraction solution chloroform/methanol (1:2 v/v) and homogenised, with a Polytron (Kinematica, Switzerland) for 1 min at 15 600 × g. Then, 1 mL of a saturated solution of NaCl was added and the mixture homogenised (30 s, 15 600 × g). Afterwards, 2 mL of chloroform were also added and homogenised once more (30 s, 15 600 × g). Finally, 2 mL of H_2O Milli-Q were added and homogenised for 1 min at 11 700 × g. The samples were centrifuged for 10 min, 4 °C, at 3 900 × g resulting in phase separation. The organic phase was collected for a new test tube containing anhydrous sodium sulphate and centrifuged for 3 min, 4 °C, at 3 900 × g. The lipid extract was filtered and dried through cotton and anhydrous sodium sulphate column and collected for a weighted pear flask (P_t). To wash the lipids retained in the tube containing the anhydrous sodium sulphate, 2 mL of chloroform were added, vortexed, and centrifuged for 3 min, 4 °C, at 3 900 × g. The lipid extract was collected and filtered through the column with cotton and anhydrous sodium sulphate. This column was washed with the addition of 1 mL of chloroform 3 times. The sample was dried using a rotary evaporator at 40 °C. The remaining solvent residues were evaporated under nitrogen until constant weight (P_f). After extraction, the lipid residue was dissolved in chloroform at a final concentration of 10 mg/mL and stored at -80 °C until lipid classes analysis.

Folch method

Three millilitres of chloroform/methanol (2:1 v/v) were added to 200 mg (P_a) of macroalgae homogenate and lipids were extracted by vortexing, for 30 s, then tubes were agitated in an orbital shaker for 10 min at room temperature, at 1326 × g. Then, 3 mL of HCl 0.1 N and 300 µL of $MgCl_2$ 0.5% (w/v) were added, mixed using the vortex and centrifuged for 5 min, 4 °C, at 2000 × g, resulting in the phases separation. The lower phase (organic layer), containing the lipids, was filtered and dried through cotton and anhydrous sodium sulphate column, and collected for a weighted pear flask (P_t). Algae homogenate was extracted once more with 3 mL of chloroform/methanol (2:1 v/v) and the tubes were agitated once more in an orbital shaker for 10 min at room temperature, at 1326 × g. Lipid extracts were then centrifuged for 5 min, 4 °C, at 2000 × g, the organic phase was collected, and dried through a cotton column containing anhydrous sodium sulphate. The solvent in the lipid extracts was evaporated using a rotary evaporator at 40 °C. The remaining solvent residues were evaporated under nitrogen until constant weight (P_f). After extraction, the lipids residue was resuspended in chloroform at a final concentration of 10 mg/mL and stored at -80 °C until lipid classes analysis.

For both extraction methods, TL were quantified according to equation 3.1:

$$Total\ lipids\ (\%) = \left(\frac{P_f - P_t}{P_a}\right) \times 100 \qquad \text{(Eq. 3.1)}$$

3.6. Lipid classes determination

3.6.1. Optimization of lipid classes quantification by HPTLC

To improve the chromatographic conditions and develop a sensitive and reproducible method for the determination of lipid classes in macroalgae matrix, multiple parameters concerning the chromatographic analysis were tested and optimized. The optimization protocol followed the procedures detailed in section 3.6.2, with slight changes in order to individually test each of the studied parameters summarized in Table 3.2, however, results will be discussed further in section 4.2.1.

Table 3.2 Optimization of the HPTLC analysis: the studied parameters of each chromatography step.

Chromatography step	Studied parameter	Tested conditions
Application	Stationary phase (plates manufacturing brand)	Macherey-Nagel and Merck plates
	Band length	7, 9 and 10 mm
	Number of bands	13, 14, 15 and 19 bands
Development	Migration distance combinations for 1st and 2nd elutions	38 and 85 mm, 48 and 92 mm, 58 and 95 mm
	Chamber saturation conditions	With and without filter paper
	Mobile phase composition	KCl 0.25% w/v volume: 0.8, 1.6, 2 and 2.5 mL
Derivatization	Pigments detection	Detection before derivatization
	Derivatization solutions and method	Phosphomolybdic acid at 5 and 10% w/v (immersion and spraying), cupric acid solution (immersion), orcinol-sulphuric acid solution (spray and immersion)
	Charring time and temperature	100, 110 and 120 °C detection every 10 min until optimal detection

The optimized HPTLC method was validated concerning the following parameters: working range, precision, sensitivity (LoD and LoQ) and specificity, according to "Guia Relacre"[101].

3.6.2. Lipid classes quantification

3.6.2.1. Sample application

Before application, the pre-coated silica gel 60 F_{254} plates were marked at 48 and 95 mm from the bottom to use as a reference to control the solvent front. Samples (6-10 µL) and standards (2-12 µL) were applied as bands of 9 mm long, with a dosage syringe using the Linomat 5 device, at a constant rate of 150 nL/s. Bands were applied at 8 mm from the lower edge of the plate. A distance of 23 mm for the left/right edge was left empty. In the end, plates were left to dry for 10 minutes in the desiccator.

3.6.2.2. Development

Lipid classes separation relied on a double elution procedure, based on compounds polarity. The PL were eluted in the first place with a mobile phase consisting of a more polar mixture, while NL were eluted in second place with a less polar mixture. The PL were separated using a solvent mix of methyl acetate-isopropanol-chloroform-methanol-KCl 0.25 % (25:25:25:10:5 v/v/v/v/v) up to 48 mm[109]. After PL elution, the plates were left to dry in the fume hood for a few minutes (just enough time to evaporate most of the solvent) and then, left in a desiccator for 10 minutes. For the separation of NL, silica plates were eluted with a solvent mixture consisting of isohexane-diethyl ether-acetic acid (80:20:2 v/v/v). The length of chromatographic run was 95 mm. Once more, after elution, the plates were left to dry in the fume hood for a few minutes and then, transferred to a desiccator (10 minutes). In both elutions, once the solvents were added, the chamber was left to condition for 10 min, before introducing the plate.

3.6.2.3. Derivatization

Different derivatization procedures were followed depending on whether it was for lipid classes quantification or confirmation. Lipid classes quantification was accomplished by immersion of the developed plate in a solution of phosphomolybdic acid 5% w/v for 6 s using the Chromatogram Immersion Device 3, followed by charring for 1 h in a heating oven set to 100 °C. In turn, for GL bands confirmation, the plates were immersed in a solution of orcinol-sulphuric acid and charred for 15 min in a heating oven set to 125 °C[109,110]. The bands corresponding to GL appeared as a blue-violet colour. Phospholipids confirmation was carried out by spraying the plate with molybdenum reagent of Dittmer-Lester, revealing a blue colour[111]. As these reagents cannot be used simultaneously, different plates were applied and developed, for each derivatization protocol.

3.6.2.4. Quantification

Lipid classes quantification was carried out by densitometry. The plates were scanned with the TLC Scanner 4 (CAMAG), in the reflectance-absorbance mode at 460 nm using a deuterium lamp. The parameters for the densitometric scanning were set as follows: slit dimension of 4.00 × 0.30 mm, scanning speed of 20 mm/s, data resolution of 100 µm/step. The acquired data was then processed using the winCATS software (1.4.8.2031). Figure 3.2 shows a track with the lipid classes already separated and their correspondence with the HPTLC densitogram.

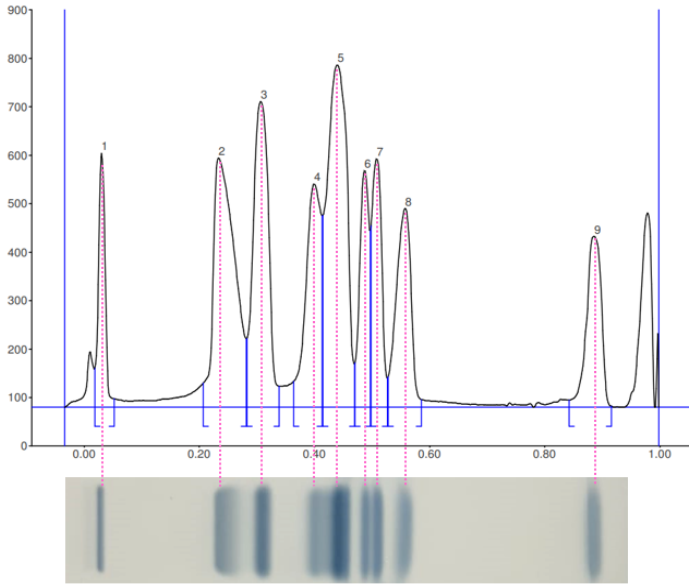

Figure 3.2 Example of chromatographic separation of a standard pool (1 mg/mL) containing: PC (**1**), SQDG (**2**), DGDG (**3**), SL (**4**), MGDG (**5**), 1,2-DAG (**6**), 1,3-DAG (**7**), FFA (**8**) and TAG (**9**). Each line corresponds to the respective compound band.

3.6.3. Validation of lipid classes determination by means of HPTLC

3.6.3.1. Specificity

The method specificity was determined based on the lipid classes retention factor (R_f) of a standard solution and their respective resolution (R_s) values (Table 3.3). If $R_s > 1.5$, then the method is considered to be specific for that lipid class. The R_s was determined as described in section 1.4.1.

3.6.3.2. Calibration curves and working range

In order to determine the working range, volumes between 2.0 – 12.0 µL of standard solution (1 mg/mL), corresponding to 2.0, 4.0, 6.0, 8.0, 10.0 and 12.0 µg, were applied in duplicate in the HPTLC plate, except for the lower (2.0 µL) and upper limits (8.0, 10.0 and 12.0 µL) that were applied ten times. To estimate the PG value, ten applications of the upper and lower limits of the

working range were considered, for each lipid class. The calibration curves, expressed as second order polynomial regressions, were determined based on the relation between the mass and peak area.

3.6.3.3. Analytical limits

The sensitivity of the method for the lipid classes determination was estimated in terms of the analytical limits LoD and LoQ. The lower mass of the calibration curve was considered as the LoQ. In turn, the LoD value was determined by dividing LoQ by 3.3[125] .

3.6.3.4. Precision

Concerning the methods precision, it was estimated in terms of repeatability and intermediate precision. Precision studies covered the entire working range. The limits of the working range (2.0 and 12.0 µg) were spotted 6 times while the intermediate points (4.0, 6.0, 8.0 and 10.0 µg) were spotted in triplicate. The plates were scanned 6 times. To assess the intra-day variation, the precision of the method was ascertained by analysing lipid classes standard solutions (within the same points as working range) two times on the same day. On the other hand, intermediate (inter-day) precision was determined by analysing the standard solution on two different days under the same experimental conditions.

3.7. Fatty acid profile assessment

The determination of the FA profile of algal biomass was performed as described by Lepage & Roy[112] with some modifications as described by Bandarra *et al.*[113]. Five millilitres of freshly prepared acetyl chloride:methanol (1:19 v/v) and 10 µl of internal standard (21:0) were added to 300 mg of sample. The tubes were vortexed for 30 seconds and were left to react in a water bath adjusted to 80 °C for 1 h. The tubes were cooled for 30 min at room temperature. Then, 1 mL of Milli-Q water and 2 mL n-heptane were added, and the tubes vortexed once more. The fatty acids methyl esters (FAME) extract was then centrifuged for 3 min, 3 000×g. The upper phase, containing heptane and FAME, was filtered through a column with cotton and sodium sulphate anhydrous to a vial and stored at -80 °C until further analysis.

The quantification of FAME was accomplished by flame-ionization gas chromatography (GC-FID) using a Scion 456-GC gas chromatograph, with a capillary polyethylene glycol DB MAX column (30 m × 0.25 mm i. d., 0.25 µm film thickness) and helium as the carrier gas. A volume of 2 µL of the sample was auto injected. The FAME separation was carried out using a temperature program for the column starting at 180 °C, increasing to 200 °C at 4 °C/min, holding for 10 min at 200 °C, heating to 210 °C at the same rate, and holding at this temperature for 14.5

min. The FAME identification was based on their retention time, using a standard mix (PUFA-3, Menhaden oil, Sigma-Aldrich) as reference.

The quantification was based on the internal standard method. After a prospective trial, and considering that heneicosanoic acid (21:0) was absent in the macroalgae samples, it was used as an internal standard at a concentration of 10 mg/mL (prepared by dissolving 100 mg of pure standard in 10 mL n-heptane). Analysis was performed in duplicate, for each sample, and the results expressed both as relative content of total FA as well as in mg/100 g on a dw basis.

3.8. Fatty acid composition of PL classes

A deeper characterization of macroalgae PL fraction was carried out by means of preparative thin layer chromatography (PTLC).

3.8.1. Optimization of PTLC procedures

Similar to what happened with the analysis of lipid classes by HPTLC, some of the PTLC procedures were also tested and optimized. In global terms, the separation of PL classes followed the procedures explained in the section 3.8.2, with slight modifications in order to evaluate the studied parameters summarized in Table 3.4, in order to get the best separation possible of the PL classes. The parameters tested will be discussed further in section 4.2.3.

Table 3.4 Optimization of the PTLC analysis: the studied parameters of each chromatography step.

PTLC Step	Studied Parameters	Tested conditions
Application	Plate type	HPTLC plates (0.5 mm thickness) and preparative plates (2 mm thickness)
	Band length	5, 10, 18 and 20 mm
	Sample volume	20, 50, 75, 100 and 150 µL
	Concentration of the extract	10, 30 and 50 mg/mL
Derivatization	Optimal detection for scraping	Dichlorofluorescein 0.2% and orcinol-sulphuric acid solutions

3.8.2. Purification of the PL fraction

In order to minimize interferences from NL and pigments, a previous cleaning step was required, for the successful separation of lipid classes. The PL fraction purification followed the procedures described in Cyberlipid website[114]. Firstly, the SPE column was rinsed with 2 mL of chloroform. After the solvent level has dropped to the top of the gel, 200 µL of lipid extract (10 mg/mL) was

applied to the column. The NL lipids were eluted in first place with 10 mL of chloroform. Then, 15 mL of acetone/methanol (9:1 v/v) were added to elute GL and SL. In the end, 10 mL of methanol were added to elute the phospholipids fraction. The solvents were completely drained before adding a different mobile phase. Afterwards, the solvent was evaporated until dryness and resuspended in chloroform at a final concentration of 30 mg/mL.

Fifty microliters of purified extract were applied using the Linomat 5 as 18 mm wide bands (7 bands, 350 µL/plate), in a Silica gel 60 F_{254} HPTLC glass plate (200 x 100 mm, 0.5 mm thickness). Lipid classes separation was accomplished in a glass chromatography chamber, as previously described, using a solvent mix of methyl acetate-isopropanol-chloroform-methanol-KCl 0.25 % (25:25:25:10:5 v/v/v/v/v) up to 85 mm. The plates were then split into two fragments: one smaller (corresponding to one track) that was derivatized and used as a reference and the other fragment with the remaining tracks. The comparison of both fragments enabled to identify the bands positioning as shown in Figure 3.3, leaving the remaining plate intact for scrapping and further processing. This is an important aspect since after the derivatization with orcinol FA cannot be used for FAME analysis. For each sample, 3 plates were used, and the corresponding bands were pooled together, in tubes, for each lipid class (assigned with 1, 2, 3, and 4, as represented in Figure 3.3).

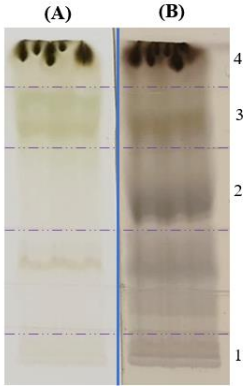

Figure 3.3 Comparison of the non-derivatized **(A)** and the derivatized **(B)** plates and respective bands delimitation: PC **(1)**, PE+SQDG **(2)**, DGDG **(3)**, MGDG **(4)**.

For each lipid class, and respective portion of silica scraped from the plate, the FA profile was determined as described in section 3.7. However, in this case, no internal standard was used. Analysis were carried out in duplicate and the results expressed as relative content of total FA.

3.9. Statistical analysis

The data were tested for statistical outliers using the Grubbs test, using the SPSS Version 23 (SPSS Inc., Chicago, U.S.A.). To test the data normality and homogeneity of variance, Kolmogorov-Smirnov's test and Levene's F-test, respectively, were used. Since these parameters

were confirmed, the analysis of variance Factorial ANOVA using Statistica™ v.12 software (StatSoft Inc, U.S.A.) was carried out. The TL extraction protocol, macroalgae species and processing were the factors used for the statistical analysis. Means were compared, and significant differences ($p < 0.05$) were determined according to Tukey's Honest Significant Differences (HSD) test. Pearson's correlations were also calculated for a significance level of $p < 0.05$.

4. Results and Discussion

4.1. Total lipids content

Due to the importance of lipids and FA, reliable methods are required for the extraction of these compounds, namely, from macroalgae matrix. Firstly, the present study aimed to evaluate and compare the lipid content of selected macroalgae species when different analytical protocols were followed. As such, the lipid fraction of the red algae, *A. armata* and *A. taxiformis*, and the brown algae, *C. humilis* and *T. abies-marina*, was extracted according to Folch and Bligh and Dyer methods. The effect of the extraction protocol and drying processes were also evaluated in terms of TL content. The results regarding the TL content (expressed in % dw) are presented in Figure 4.1.

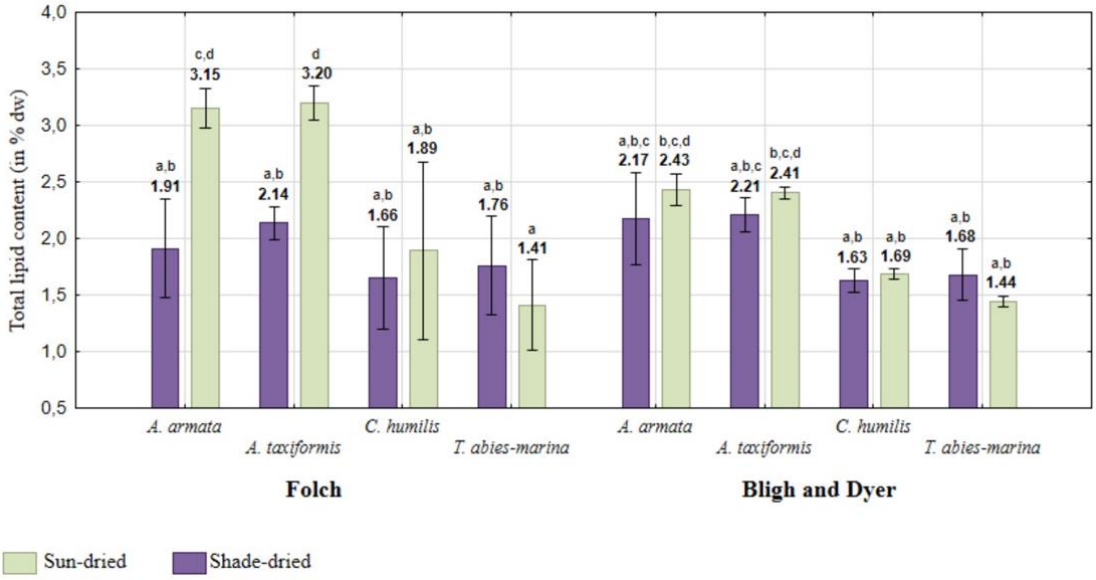

Figure 4.1 Average TL content of studied macroalgae, determined by Folch and Bligh and Dyer methods (expressed in % dw). Error bars correspond to standard deviation. Different letters correspond to significantly different arithmetic means ($p < 0.05$) (n = 3).

In global terms, the TL contents ranged between 1.41 and 2.43% dw found in shade-dried *T. abies-marina* (Folch method) and sun-dried *A. armata* (Bligh and Dyer method), respectively. These results did not vary significantly within the considered species, the drying condition, or the extraction protocol. The sun-dried red algae, extracted according to the Folch method, were the exception, with significant higher lipid contents: 3.15 and 3.20% dw (registered for *A. armata* and *A. taxiformis*, respectively), in opposition to shade-dried counterparts that exhibited 1.91 and 2.14% dw (found in *A. armata* and *A. taxiformis*, respectively). Although these results were unexpected, a similar trend was also described by Regal *et al.*[40] in *A. taxiformis* harvested in a

different period (November 2018). These authors have also reported differences in TL content as a result of different drying processes: 3.4% dw for freeze-dried samples, comparing with 1.5% dw for oven-dried samples. This suggests that different drying conditions may lead to shifts within the macroalgae matrix, favouring the extraction of other liposoluble compounds besides lipids. The sun-dried *Asparagopsis* TL, determined according to Bligh and Dyer, also seem to exhibit a similar trend, with slightly higher contents, yet no statistically significant differences were observed ($p > 0.05$). When this analytical protocol was used, *A. armata* TL contents corresponded to 2.17 and 2.43% dw (shade and sun-dried, respectively), while *A. taxiformis* had 2.21 and 2.41% dw (shade and sun-dried, respectively). However, in the Folch method, irrespective of the species, shade-dried macroalgae showed consistent values, for instance, 1.91 and 2.14% dw (*A. armata* and *A. taxiformis*, respectively). The TL determined in brown macroalgae was slightly ($p > 0.05$) lower, when compared to red algae samples. *C. humilis* TL contents ranged from 1.63 to 1.89% dw (shade-dried extracted by Bligh and Dyer and sun-dried extracted by Folch methods, respectively), while *T. abies-marina* varied between 1.41 and 1.76% dw (sun- and shade-dried extracted by Folch method, respectively).

Apart from the mentioned differences regarding red macroalgae, the results of the present study emphasize that Bligh and Dyer and Folch methods did not lead to significant differences in TL extraction. This was expectable, based on what was previously described in Iverson *et al.*[115] work where, for samples with less than 2% of lipid content, the results of TL using the Bligh and Dyer method did not differ from those extracted by the Folch method. Even though this limit was slightly surpassed in red macroalgae, no divergences were found in results produced by these two methods. Concerning the selected macroalgae TL contents, the differences in extraction methods used in the available literature, difficult the comparison of the results found in the present study. According to Gosch *et al.*[116], Ochrophyta are the algae that usually have higher levels of TL, when compared to Rhodophyta and Chlorophyta. In fact, Wielgosz-Collin *et al.*[27] refer that TL content could vary up to 20% in the brown algae *Dictyota sandvicensis*. Gosch *et al.*[116] also observed a considerable variation in TL between orders and species, at lower taxonomic levels. Nonetheless, this variation was not confirmed in the present study, neither brown algae displayed higher TL levels. The season is often referred to as an important factor regarding macroalgae TL contents. Honya *et al.*[117], for instance, observed minimal TL content from April to June. Besides, studies undertaken with other brown macroalgae (*Sargassum horneri*, *C. hakodatensis* and *Fucus vesiculosus*), by Nomura *et al.*[118] and Costa *et al.*[31], found higher values of TL in winter (beginning in October or November and reaching a maximum in January/February, decreasing thereafter). The macroalgae *C. humilis* and *T. abies-marina* that were used in the present study were collected in April, which could explain the lower TL. According to Vizetto-Duarte *et al.*[48] and Moreno *et al.*[119], TL content of *C. humilis* and *T. abies-marina* corresponded to 5.22 and 8.5% dw,

respectively which were higher than the levels obtained in the present study. Likewise, Nunes *et al.*[120] determined, for *A. taxiformis*, a 5.42% dw TL content, which also revealed to be higher than those found in the current analysis.

4.2. Lipid classes determination

4.2.1. Optimization of HPTLC analysis

A set of chromatographic parameters (already presented in Table 3.2) were tested and optimized in order to establish a sensitive and reproducible method to assess the lipid classes in macroalgal matrices. Besides the selection of the best extraction method, the following chromatographic steps will be discussed: application, development and derivatization. It is also important to note that no statical analysis was performed.

4.2.1.1. Selection of the best method for polar lipids extraction

The TL extraction efficiency and accuracy may vary, mostly, according to each macroalgae species and extraction methods applied. For instance, the solubility of lipid classes in the solvents, the proportion of polar/non-polar solvent, along the nature of the non-polar solvent are characteristics that could reflect different TL contents. It is important to note that in order to obtain the best balance between PL and NL extraction, the mixture of solvents employed should be polar enough to remove lipids from their associating cell constituents, as their protein-lipid complexes, but not polar enough to prevent the solubilization of NL, such as TAG[25]. The main differences between the extraction methods considered in this study rely on the proportion of methanol and chloroform. In the Bligh and Dyer method, a mixture of chloroform/methanol 1:2 v/v was used, while in the Folch method a proportion of 2:1 v/v was used. Although different solvent proportions did not entail differences in the aforementioned TL contents, it was expected that different lipid classes would be extracted at different rates. In light of the objectives defined for this study, it was important to select the best method, that could deliver the best results in terms of PL, and particularly of GL. Both lipid extracts of *C. humilis*, obtained by Folch and Bligh and Dyer methods, were applied, the lipid classes determined and the lipid classes profile determined, as shown in Figure 4.2. The choice also relied on supplementary confirmation plates, that were developed and derivatized with orcinol-sulphuric acid solution to confirm GL bands. The method delivering the best results regarding PL extraction was Bligh and Dyer. The lipid extracts produced using this method enabled to obtain more intense, better defined, and individualized bands and peaks of the most important PL classes present in the selected macroalgae, namely MGDG, SQDG and DGDG (Figure 4.2 (B)). As the mixture chloroform/methanol 1:2 v/v (used in Bligh and Dyer) has a higher polar solvent proportion (methanol), the extraction of PL classes was favoured. The solvents mixture used in the Folch method (chloroform/methanol 2:1 v/v), in

turn, was more effective to extract NL lipid classes. Thus, the Bligh and Dyer method should be selected for the determination of macroalgae lipid classes.

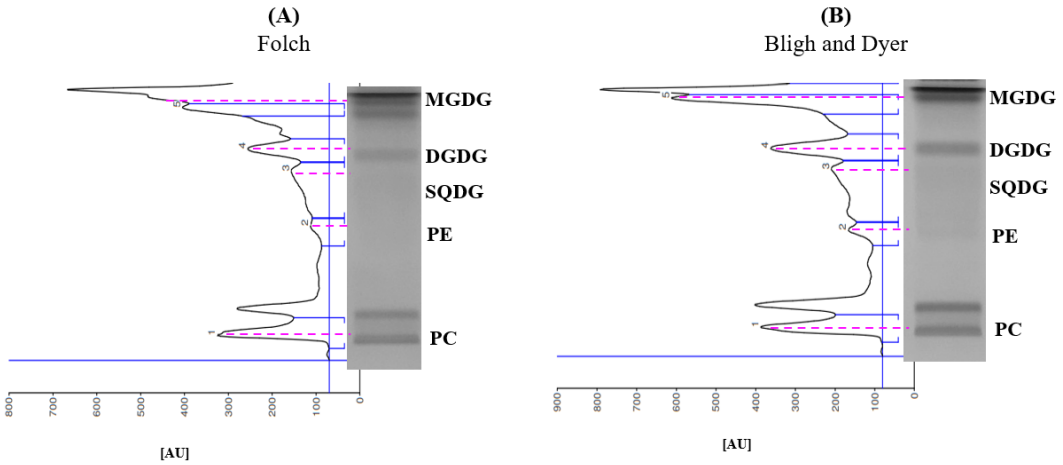

Figure 4.2 Comparison of PL classes (**PC**: phosphatidylcholine, **PE**: phosphatidylethanolamine, **SQDG**: sulfoquinovosyldiacylglycerol, **DGDG**: digalactosyldiacylglycerol, **MGDG**: monogalcatosyldiacylglycerol) obtained by both Folch **(A)** and Bligh and Dyer **(B)** methods, in sun-dried C. humilis. Plates were derivatized with a cupric acetate solution.

4.2.1.2. Sample application

Regarding sample application three parameters were taken into consideration: the plates manufacturing brand, as well as the band length and the number of tracks for each plate.

Plates manufacturing brand

For this study, two different brands were tested: Macherey-Nagel and Merck. Although no differences were perceived immediately after the sample application, they became clear after the lipid classes separation and derivatization was concluded. As can be seen in Figure 4.3, the bands applied in the Macherey-Nagel plates were poorly defined, denoting a lower resolution when compared to Merck counterparts. These findings were noticed both for standards and macroalgae samples. For these reasons, Merck plates were selected for further analysis.

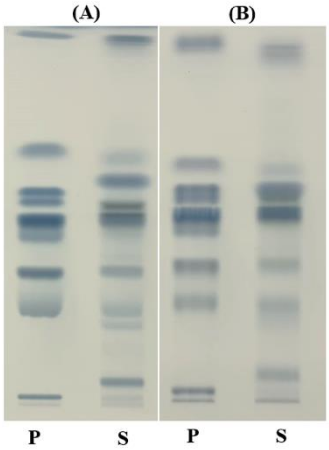

Figure 4.3 Comparison of lipid classes separation obtained with both Merck **(A)** and Macherey-Nagel **(B)** plates, in which P refers to a pool of standards (containing PC, SQDG, DGDG, SL, MGDG, 1,2 DAG, 1,3 DAG, FFA and TAG) at 1 mg/mL. "S" designates the application of shade-dried *T. abies-marina* at 10 mg/mL. Plates were derivatized with phosphomolybdic acid at 5% w/v.

Band length and number of tracks

Regarding the optimal bands size evaluation, three lengths were considered: 7, 9 and 10 mm. The smaller bands were thicker, leading to a greater bands diffusion, particularly on bands corresponding to FFA, which are, usually, larger and more diffused as observed below, in Figure 4.4.

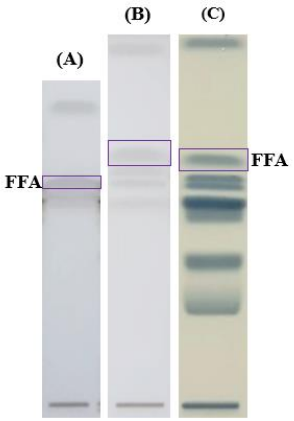

Figure 4.4 Comparison of lipid classes separation obtained for bands with 7 mm **(A),** 9 mm **(B)** and 10 mm **(C)** applications of a pool of NL standards (**(A)** and **(B)**), constituted by MAG, 1,2 DAG, 1,3 DAG, FFA and TAG at 1 mg/mL and NL and polar standards (**(C)**), constituted by PC, SQDG, DGDG, SL, MGDG, 1,2 DAG, 1,3 DAG, FFA and TAG at 1 mg/mL. Both **(A)** and **(B)** plates were derivatized with a cupric acetate solution and plate **(C)** was derivatized with phosphomolybdic acid 5% w/v.

The increase to 9 mm resulted in a band definition improvement, as well as better peak resolution in the respective densitograms. In turn, the increase for 10 mm showed no benefits, which led to fix the 9 mm length as the ideal.

Naturally, the number of tracks in each plate is directly related to the band length. Once more, having in mind the bands definition and peaks resolution improvement, another test was performed with plates with 15, 14 and 13 bands. The best results were delivered by plates containing 13 tracks, 9 mm each.

4.2.1.3. Development

Regarding development, different parameters were taken into consideration, namely, the mobile phases migration distance, the composition of the first mobile phase (to elute PL) and chamber saturation conditions.

Concerning the migration distance of the solvent front, different measures were considered for the first and for the second mobile phases (that elute PL and NL, respectively): 48 and 85 mm, 58 and 85 mm, 38 and 92 mm and 48 and 95 mm. These experiments aimed to improve the separation of pigments, SL, MGDG, 1,2 DAG, 1,3 DAG and FFA. The initial conditions of the development were 48 mm of migration for the first elution, followed by 85 mm for the second elution. The first test consisted of increasing the polar development migration distance to 58 mm (second elution up to 85 mm), which did not show any improvements, as the 27 mm left between the polar and non-polar solvent fronts were not enough to separate NL. The following test, consisted of the decrease of this distance to 38 mm, along with the increase of second elution migration for 92 mm. In this case, despite an improved DAG resolution, the SQDG definition was lost, which was not a viable option due to this compound relevance in the present study. The best results were obtained with the PL development up to 48 mm and the NL development up to 95 mm. For being a larger and diffuse band, these elutions distances enabled to fix FFA in a higher R_f and improve this lipid class separation.

After the migration distances adjustments, different KCl 0.25% w/v solution volumes (in PL mobile phase) were tested, to improve PL bands resolution, for instance, in SQDG. For this reason, the mobile phase initial composition in KCl solution (0.8 mL) was adapted, and the addition of higher volumes (1.6, 2.0, and 2.5 mL) was evaluated (Figure 4.5). The increase in KCl 0.25% w/v solution volume from 0.8 to 2 mL, lead to an increase of the solution ionic strength and, consequently, allowed an improved band definition, in comparison with the other volumes tested, namely, 0.8, 1.6, and 2.5 mL. Cañavate *et al.*[109] also observed that an increase in KCl 0.25% w/v volume, improved bands resolution. Furthermore, narrower bands were also observed as a result of higher levels of KCl 0.25% w/v.

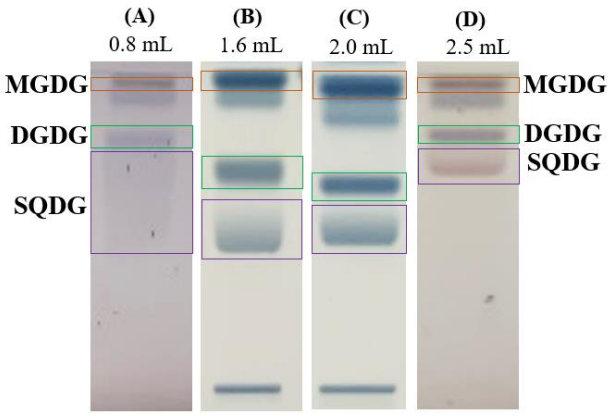

Figure 4.5 Comparison of bands resolution when different volumes of KCl 0.25% w/v were tested. **(A)** and **(D)** are GL confirmation plates (derivatized with an orcinol-sulphuric acid solution) and **(B)** and **(C)** are quantification plates (derivatized with phosphomolybdic acid 5% w/v).

The use of filter paper is often used as a way to improve the chamber saturation. Another experiment was carried out, to evaluate the effect of the filter paper, however, no differences were observed in bands resolution neither in reproducibility. In view of this, the filter paper was no longer used.

4.2.1.4. Derivatization/Detection

The derivatization protocol already implemented at IPMA relied on spraying the plates with phosphomolybdic acid 5% w/v. This procedure proved to cause interferences and significant noise, diminishing bands resolution, and making lipid classes identification and quantification more challenging. As such, tests involving different derivatization methods were undertaken. These included the immersion in different derivatization solutions: phosphomolybdic acid solution at 5% w/v, phosphomolybdic acid solution at 10% w/v, and cupric acetate solution as described by Cañavate *et al.*[109].

The derivatization by immersion with cupric acetate solution enabled to obtain a homogeneous plate, with a visible reduction of associated noise. Although, when compared to derivatization by spraying with phosphomolybdic acid 5% w/v, the bands have also lost intensity. To overcome this loss of sensitivity, other charring temperatures were studied: 100 and 120 ºC. Intermediate readings, until a maximum of 1 h, were performed: every 15 min. From these tests it was possible to conclude that plates charred at 120 ºC provided the best results, with more defined and intense bands. However, although these results were apparently better, in samples with lower GL amount derivatization with cupric acetate was not efficient enough to detect them. As more intense bands and the identification of GL and phospholipids was required, for the studied macroalgae, tests, with phosphomolybdic acid at 5% w/v, were developed. Instead of spraying, plates were immersed in the derivatizing solution using the Chromatogram Immersion Device 3 (CAMAG).

As expected, the immersion procedures, in opposition to spraying as previously used, substantially improved bands definition and reduced interferences. Bands intensity was also better when compared with cupric acetate solution. Still, other attempts to enhance bands intensity were undertaken, testing other temperatures (100 °C and 110 °C), charring times (readings every 10 min) and increasing phosphomolybdic acid concentration (from 5 to 10% w/v) (Figure 4.6).

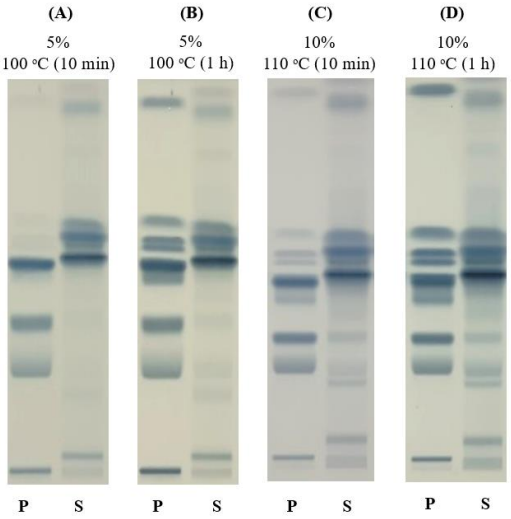

Figure 4.6 Comparison between results obtained with both 5 and 10% w/v phosphomolybdic acid concentrations and charring at 100 and 110 °C, in which P refers to a pool of standards (containing PC, SQDG, DGDG, SL, MGDG, 1,2 DAG, 1,3 DAG, FFA and TAG) at 1 mg/mL. "S" designates the application of sun-dried *T. abies-marina* at 10 mg/mL.

Although the derivatization with a 10% w/v phosphomolybdic acid solution promoted more intense bands (with a shorter reaction time in the oven (Figure 4.6 (C)), there was also a noise increment, which difficult the identification of less intense bands with a good resolution (Figure 4.6 (D)). In the end, the best results for quantification plates were achieved by immersion in phosphomolybdic acid 5% w/v and charring at 100 °C for 1h (Figure 4.6 (A)).

4.2.2. Validation of lipid classes determination by means of HPTLC

The optimized analytical protocol was then validated in terms of specificity, working range, analytical limits and precision. Even though other criteria are included in the typical validation procedures, these are the parameters most commonly considered for validation analytical protocols based in HPTLC[102,121–124]. Each parameter will be discussed in the following sections.

4.2.2.1. Specificity

The HPTLC plate used for specificity determination is represented in Figure 4.7, along with the R_s values determined for each lipid class, in Table 4.1.

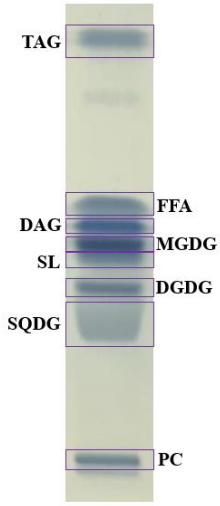

Figure 4.7 HPTLC plate spotted with lipid classes standards at 1 mg/mL, derivatized with a phosphomolybdic acid 5% w/v solution.

Table 4.1 Specificity of the HPTLC method optimized for lipid classes quantification.

Lipid class	Max R_f	End R_f − Max R_f	R_s
PC	0.03	0.04	4.00
SQDG	0.29	0.09	0.86
DGDG	0.35	0.05	1.50
SL	0.41	0.03	0.57
MGDG	0.43	0.04	1.00
DAG	0.47	0.04	0.89
FFA	0.51	0.05	5.82
TAG	0.83	0.06	1.86

In view of these results, it is possible to conclude that the optimized method was specific for TAG, PC and FFA as the R_s was above 1.5 for these lipid classes (1.86, 4.00 and 5.82, respectively). Regarding SQDG, DGDG, SL, MGDG and DAG, notwithstanding individual bands were visualized in the plate (Figure 4.7), they were quite close to each other, which explains the lower R_s. Regardless, the analysis of the corresponding densitogram shows that bands separation was enough to allow a correct identification and quantification of the lipid classes.

4.2.2.2. Calibration curves and working range

The calibration curves, expressed as second order polynomial regression and the respective correlation coefficients are presented in Table 4.2.

Table 4.2 Calibration curves and working range data determined for the HPTLC method optimized for lipid classes quantification.

Lipid class	Working range	Equation	R^2	PG
PC	2.0 – 12.0 µg	$y = -41.7x^2 + 1095.1x + 265.6$	0.999	1.5
SQDG	2.0 – 12.0 µg	$y = -67.0x^2 + 1891.3x + 109.8$	0.996	2.8
DGDG	2.0 – 12.0 µg	$y = -38.1x^2 + 1367.0x + 2159.5$	0.998	2.0
SL	2.0 – 10.0 µg	$y = -47.5x^2 + 1043.4x + 1620.7$	0.993	2.8
MGDG	2.0 – 12.0 µg	$y = -51.5x^2 + 1722.0x + 6348.8$	0.990	2.2
DAG	2.0 – 12.0 µg	$y = -118.2x^2 + 2284.0x + 2211.2$	0.992	1.1
FFA	2.0 – 8.0 µg	$y = -169.7x^2 + 2477.8x - 196.6$	0.999	1.5
TAG	2.0 – 12.0 µg	$y = -45.1x^2 + 1035.5x + 1940.5$	0.990	1.0

The correlation coefficient ranged from 0.990 to 0.999 ($r^2 \geq 0.990$). The lipid classes within the acceptance criteria ($r^2 > 0.995$), as proposed in Guia Relacre[101], were PC, SQDG, DGDG and FFA showing a good correlation between the mass and the peak area. Instead, SL, MGDG, DAG and TAG were below the acceptance criteria considered. Still, these lipid classes showed a strong correlation, following the acceptance criteria considered by Masota *et al.*[123] ($r^2 > 0.980$). Moreover, the comparison between PG test values and the Snedecor-Ficher F distribution table value ($F = 3.179$, for 9 degrees of freedom and $p < 0.05$), shows that the condition $PG \leq F$ is confirmed, indicating that the selected working range is well suited for this method, irrespective of the considered lipid class. It should also be highlighted that the initial working range for FFA and SL (2.0 – 12.0 µg), had to be reduced in order to observe this assumption ($PG \leq F$).

4.2.2.3. Analytical limits

The sensitivity of the method for the lipid classes determination was estimated in terms of the analytical limits LoD and LoQ. The LoQ was defined as based in the lower mass standard of the calibration curve, thus 2.0 µg. In turn, the LoD value was determined was 0.6 µg.

4.2.2.4. Precision

The results are presented and expressed in terms of relative standard deviations (%RSD), in Table 4.3.

Table 4.3 Precision of the HPTLC method developed for lipid classes determination.

Lipid classes	Parameter	Repeatability		Intermediate precision
		Intra-day (day 1)	Intra-day (day 2)	Inter-day (day 1 and 2)
PC	Peak areas mean	1496.9 ± 48.2	1442.5 ± 47.6	1469.7 ± 54.2
	%RSD	3.2	3.3	3.7
SQDG	Peak areas mean	2786.2 ± 83.5	1687.3 ± 76.4	2236.7 ± 70.7
	%RSD	3.0	4.5	25.5
DGDG	Peak areas mean	2468.4 ± 64.9	2036.2 ± 111.3	2252.3 ± 239.3
	%RSD	2.6	5.5	10.6
SL	Peak areas mean	3189.5 ± 80.8	2548.0 ± 148.0	2868.8 ± 349.8
	%RSD	2.5	5.8	12.2
MGDG	Peak areas mean	7475.3 ± 267.2	7078.1 ± 168.6	7276.7 ± 297.9
	%RSD	3.6	2.4	4.1
DAG	Peak areas mean	5674.9 ± 109.6	5701.6 ± 129.8	5688.3 ± 117.4
	%RSD	1.9	2.3	2.1
FFA	Peak areas mean	2764.6 ± 250.8	5185.8 ± 94.3	3975.2 ± 1259.2
	%RSD	9.1	1.9	31.7
TAG	Peak areas mean	3212.8 ± 149.6	3399.7 ± 67.6	3306.2 ± 148.1
	%RSD	4.7	2.0	4.5

As shown in Table 4.3, the results regarding the intra-day precision (repeatability) were, in general terms, lower than 5%, indicating a good precision of the optimized method. In fact, in what concerns to TLC densitometry, %RSD values ranging from 1 to 5% are considered as acceptable[121]. Some exceptions were found, however, for FFA (9.1%, day 1), SL (5.8%, day 2) and DGDG (5.5%, day 2) denoting an %RSD higher than 5%. A similar scenario was found, for the same lipid classes, in terms of the method intermediate precision. In fact, FFA (31.7%), SL (12.2%), and DGDG (10.6%) denoted a higher variation degree, surpassing, the limit of 5%. Likewise, SQDG also had the higher %RSD (25.5%) resulting from analysis carried out on different days. The PC, MGDG, DAG and TAG were the lipid classes that showed acceptable %RSD values for the precision analysis, in terms of both repeatability and intermediate precision. Thus, it was possible to conclude that the HPTLC method that was followed was precise for analysis within the same day, for all the lipid classes studied, excluding FFA. For inter-days analysis peak areas, %RSD values results may suffer variations for some of the studied lipid classes.

4.2.3. Optimization of PL fractionation by PTLC

Even though PLC was already implemented at IPMA[51], this protocol had never been applied to GL and had never made use of the HPTLC system. For this reason, the analytical protocol for PTLC was implemented and optimized. To accomplish this, different parameters regarding sample application and bands identification were tested.

Sample application

In PTLC, compounds are separated and then scraped from the plate to be further analysed. As such, a good separation of the GL bands is mandatory to successfully fractionate MGDG, DGDG and SQDG, so they can be analysed in terms of their FAME composition. To accomplish this, some parameters were studied namely: the type of plate, the band length, along with the sample volume applied for track, and the sample concentration.

Both 100 x 200 mm HPTLC plates (0.5 mm thickness) and 200 x 200 mm PLC plates (2.0 mm thickness) plates were tested for the sample application. Applications of 20.0, 50.0, 75.0, 100.0 and 150.0 µL were tested in HPTLC plates. On the other hand, the application of 50.0 µL was tested in PLC plates. It was observed, however, that bands were poorly resolved and defined whenever PLC plates were used. On the contrary, the utmost resolution and definition were achieved when samples were applied in HPTLC plates. This is in accordance with studies that described the main differences between TLC and HPTLC plates. Srivastava[84] stated that there was a clear advantage in using a smaller average particle size of silica gel in the preparation of TLC plate height. Besides, Attimarad[126] described that better resolution was allowed by the use of higher quality TLC plates (with finer particle sizes).

Having in mind that the best option relies on a balanced compromise between the sample volume, the sample concentration, and the band length, to isolate the GL for further analysis by GC, different band lengths tested varied from 5 up to 20 mm, along with sample volumes from 20 up to 150 µL. When 150 µL macroalgae sample (10 mg/mL) was applied in 5 mm long tracks, the excessive amount of sample promoted plate saturation and, consequently, the compounds could not be separated as defined bands. On the other hand, it was observed that a 50 µL sample (10 mg/mL) application in form of 10 or 18 mm bands was not sensible enough for detection and consequent scraping. Also, when a sample concentration of 50 mg/mL was used, a mass overloading was noticed, resulting in an excessive dragging of both SQDG and DGDG bands. To overcome this issue, macroalgae lipids extract samples were purified using an SPE (section 3.8.2) and polar lipids fraction (GL and phospholipids) were collected and used in further PTLC experiments. This enabled to remove carotenoids and NL and improve the separation of SQDG

and DGDG (Figure 4.8). In the end, a 30 mg/mL of purified lipids was the concentration delivering the best results.

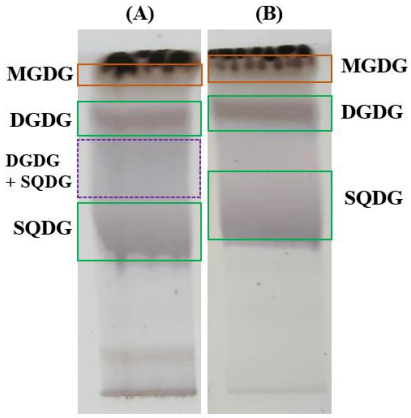

Figure 4.8 Comparison between 50 µL sample application of non-purified (50 mg/mL) **(A)** and purified (10 mg/mL) **(B)**, in GL fraction. The plate was derivatized with an orcinol-sulphuric acid solution.

Bands identification

Different derivatization reagents were tested to determine the most sensible method to identify target compounds for scrapping and consequent detection in GC analysis. The use of dichlorofluorescein is often considered as a good derivatization reagent in what concerns to PLC, once it stains the lipids without destroying them. However, this derivatization reagent proved to be poorly sensitive: only SQDG and PC could be observed. Alternatively, the orcinol-sulphuric acid solution was tested, but in order to keep the compounds intact for further analysis, the plate was cut, removing one portion of the plate (corresponding to one track). Only this small portion of the plate was derivatized and used as a reference to identify the PL bands, allowing to scrap them.

4.2.4. Lipid classes quantification by HPTLC

The lipid classes identified in the selected macroalgae and respective drying are presented at Table 4.4 (expressed in % of TL).

Table 4.4 Lipid classes profile determined in selected macroalgae species, and both drying conditions (expressed in % of TL).

	A. armata		***A. taxiformis***		***C. humilis***		***T. abies-marina***	
	Sun-dried	Shade-dried	Sun-dried	Shade-dried	Sun-dried	Shade-dried	Sun-dried	Shade-dried
PC	8.9 ± 1.4^{b}	12.7 ± 1.9^{c}	$10.8 \pm 0.6^{b,c}$	$11.5 \pm 1.2^{b,c}$	2.7 ± 0.1^{a}	2.3 ± 0.3^{a}	2.1 ± 0.1^{a}	2.0 ± 0.2^{a}
PE	$2.9 \pm 0.3^{a,b}$	2.8 ± 0.7^{a}	$3.8 \pm 0.0^{b,c}$	$3.2 \pm 0.0^{a,b}$	5.4 ± 0.3^{d}	$3.8 \pm 0.3^{b,c}$	4.3 ± 0.2^{c}	2.3 ± 0.3^{a}
SQDG	$8.4 \pm 0.3^{c,d}$	14.3 ± 0.8^{f}	$8.9 \pm 0.5^{c,d}$	$13.5 \pm 1.0^{e,f}$	$11.1 \pm 1.9^{d,e}$	$7.7 \pm 0.8^{b,c}$	$5.0 \pm 0.1^{a,b}$	3.9 ± 1.7^{a}
DGDG	8.0 ± 0.6^{b}	$14.2 \pm 1.5^{c,d}$	$11.3 \pm 0.3^{c,d}$	$10.4 \pm 0.4^{b,c}$	16.9 ± 0.8^{e}	$8.9 \pm 0.5^{b,c}$	$7.4 \pm 1.5^{a,b}$	4.7 ± 1.7^{a}
SL	ND[1]	ND	ND	ND	ND	ND	ND	ND
MGDG	50.0 ± 0.8^{d}	33.3 ± 0.4^{c}	51.7 ± 1.7^{d}	36.7 ± 0.4^{c}	18.3 ± 0.8^{a}	23.6 ± 1.4^{b}	33.8 ± 1.0^{c}	36.6 ± 2.1^{c}
DAG	12.2 ± 0.5^{b}	12.2 ± 0.2^{b}	10.8 ± 0.7^{b}	9.1 ± 0.4^{a}	17.7 ± 0.3^{c}	22.1 ± 0.5^{e}	19.9 ± 0.5^{d}	$19.1 \pm 0.9^{c,d}$
FFA	$3.7 \pm 1.0^{b,c}$	$5.5 \pm 0.2^{a,c}$	2.6 ± 0.7^{a}	$7.3 \pm 1.1^{c,d}$	5.3 ± 0.3^{b}	7.7 ± 0.3^{d}	16.2 ± 0.6^{e}	17.1 ± 1.0^{e}
TAG	5.7 ± 0.6^{b}	$5.2 \pm 0.7^{a,b}$	ND	$8.5 \pm 0.5^{b,c}$	22.7 ± 0.0^{e}	23.8 ± 3.8^{e}	$11.3 \pm 0.6^{c,d}$	14.2 ± 3.4^{d}
∑GL[2]	**66.4 ± 0.2^{d}**	**61.8 ± 1.7^{c}**	**72.0 ± 1.6^{e}**	**60.5 ± 0.6^{c}**	**46.3 ± 0.3^{c}**	**40.2 ± 2.7^{a}**	**46.2 ± 0.6^{b}**	**45.2 ± 2.1^{b}**
∑Phospholipids[3]	**11.9 ± 1.5^{c}**	**15.5 ± 1.5^{d}**	**14.7 ± 0.6^{d}**	**14.6 ± 1.1^{d}**	**8.1 ± 0.2^{b}**	**$6.1 \pm 0.5^{a,b}$**	**$6.5 \pm 0.2^{a,b}$**	**4.4 ± 0.4^{a}**
∑PL[4]	**78.3 ± 1.7^{d}**	**77.3 ± 0.5^{d}**	**86.6 ± 1.1^{e}**	**75.1 ± 1.2^{d}**	**54.4 ± 0.6^{c}**	**46.4 ± 3.2^{a}**	**$52.6 \pm 0.5^{b,c}$**	**$49.6 \pm 1.7^{a,b}$**
∑NL[5]	**21.7 ± 1.7^{b}**	**22.7 ± 0.5^{b}**	**13.4 ± 1.1^{a}**	**24.9 ± 1.2^{b}**	**45.6 ± 0.6^{c}**	**53.6 ± 3.2^{e}**	**$47.4 \pm 0.5^{c,d}$**	**$50.4 \pm 1.7^{d,e}$**

Values are presented as average ± standard deviation. Different lowercase letters within a row correspond to significant statistical differences ($p < 0.05$).
[1]ND - not detected; [2] compromises: SQDG, DGDG and MGDG; [3] compromises: PC and PE; [4] compromises: PC, PE, SQDG, DGDG and MGDG; [5] compromises: DAG, FFA and TAG.

In the present study, significant differences were observed between the red and brown macroalgae lipid classes profile: PL were significantly higher in red macroalgae (corresponding to more than 75.1% of TL), whereas in brown macroalgae it was observed a balanced proportion between PL and NL (accounting, in mean, 51 and 49%, respectively). The sum of the PL fraction varied between 46.4% (shade-dried *C. humilis*) and 86.6% (sun-dried *A. taxiformis*). The higher contribution of PLwas observed as follows: sun-dried *A. taxiformis* (86.6%) > sun-dried *A. armata* (78.3%) > shade-dried *A. armata* (77.3%), revealing that, for these macroalgae, most of the found lipids are structurally bound in membranes. Within the PL determined in red macroalgae, GL and phospholipids, accounted in average for 65 and 14% of TL, respectively. In turn, in brown macroalgae, GL and phospholipids represented about 44 and 6% of TL, respectively. Regarding NL, higher relative contents were determined in brown macroalgae, varying from 45.6 to 53.6% (sun- and shade-dried *C. humilis*, respectively). In red macroalgae, NL found values corresponded between 13.4 and 24.9% (in sun- and shade-dried macroalgae *A. taxiformis*, respectively). Kumar *et al.*[8] found, in both red macroalgae *Gracilaria folifera* and *G. edulis*, similar levels of NL, GL, and phospholipids to those determined in the present study for *Asparagopsis*. The differences between the distribution of PL and NL, between red and brown macroalgae, could be related to the fact that these macroalgae belong to different phyla. Moreover, these differences could have been triggered by the extraction of different parts of the macroalgae, leading to different lipid

classes proportions. It was already reported in a study by Khotimchenko and Kulikova[127], in *Laminaria japonica*, that higher levels of SQDG, DGDG, and MGDG occur in the upper parts of the thallus and decrease in the lower parts. In macroalgae, GL are affected by different nutrient availability: for instance, cells do accumulate GL in the deprivation of nitrogen and phosphorus, whereas the absence of phosphate lead to an increase in SQDG and DGDG levels[67,68].

Irrespective of the macroalgae considered or drying condition employed, MGDG was predominant, in both red and brown macroalgae, but particularly in sun-dried *A. armata* (50.0%) and *A. taxiformis* (51.7%). These results are in accordance with literature, which points MGDG as the most abundant PL in algae[128,129]. Although its dominance, in *C. humilis*, the observed MGDG amount (18.3 and 23.6%, in sun- and shade-dried samples, respectively) was below the amounts stated in literature (26-47% of TL), for brown macroalgae[9]. The relative content of DGDG varied from 4.7 (shade-dried *T. abies-marina*) to 16.9% (sun-dried *C. humilis*), while SQDG ranged from 3.9 (shade-dried *T. abies-marina*) to 14.3% (shade-dried *A. armata*), respectively. Lower levels of DGDG and SQDG were also found in brown algae *Costaria costata* (5.3 and 10.6%, respectively), harvested in April, and in brown algae *U. pinnatifida* (8.4 and 10.0%, respectively), harvested in March[130,131].

The differences regarding PL composition found in this study may be related to temporal changes in winter, meaning that each macroalgae species may have different mechanisms to adapt, for instance, to low light intensity, low irradiance, or shorter day length, leading to different polar lipid compositions. For example, under low light intensity, GL from chloroplasts membranes, increase mainly due to thylakoids membrane adaptation for the maintenance of photosynthetic processes, namely, to improve light absorption and its utilization[31,131]. Besides, PL content, including GL, may vary according to the algal developmental stage, as it was found by Gerasimenko *et al.*[130] to be higher in the tissues of juvenile brown algae *U. pinnatifida*. Literature refers that the GL are found in balanced proportions of MGDG, DGDG, and SQDG, in red macroalgae[8], which, in this case, was only observed in DGDG and SQDG. The quantitative order of particular GL classes was as follows: MGDG > SQDG > DGDG, in both sun- and shade-dried *A. armata* and shade-dried *A. taxiformis* and MGDG > DGDG > SQDG in sun-dried *A. taxiformis* and both sun- and shade-dried *C. humilis* and *T. abies-marina*. It is worth to mention that in sun-dried *Asparagopsis* (except for *A. taxiformis* DGDG), the proportion of SQDG and DGDG almost halved when compared with shade-dried algae. These lower levels of both SQDG and DGDG went together with higher MGDG amounts. However, in brown macroalgae, it was observed an opposite trend: the proportion of SQDG and DGDG was higher in sun-dried macroalgae, when compared to shade-dried, along with lower MGDG contents in shade-dried macroalgae. Regarding SL, this lipid class was not detected as it is not the most common in macroalgae. In

fact, according to Kumari[128] SL is usually found in small amounts in some red macroalgae, as *G. verrucosa* and *Chondrus crispus*.

Concerning phospholipids, it was observed that PC was the most abundant in red algae, particularly, in shade-dried *A. armata* where it accounted for 12.7%. This dominance was also found in the red algae *Anfeltia tobuchiensis*, where PC accounted for 70.9% of total phospholipids[132]. In turn, PC showed a low abundance in the present brown macroalgae, around 2.0%. In fact, PE was the predominant phospholipid in brown macroalgae. The results show that PE relative contents varied, in brown macroalgae, between 2.3 and 5.4%, in shade-dried *T. abies-marina* and sun-dried *C. humilis*, respectively. It seems that PC may be a minor phospholipid in brown macroalgae species, which have been also highlighted by other works where this phospholipid was found to be absent or in low contents[27]. For example, Dembitsky *et al.*[133] did not detect PC in other macroalgae from genus *Cystoseira*, while Jones and Harwood[134] found low amounts of this phospholipid in other brown algae like *F. vesiculosus* and *Ascophyllum nodosum.* Concerning PE, it is noteworthy to mention that despite it has not been validated, it was identified in the studied macroalgae species. Since it represented an important contribution to the phospholipid fraction, those results were also included in the study of lipid classes profile. In brown macroalgae, *C. humilis*, and *T. abies-marina*, a higher contribution of PE was found for the sum of phospholipids, suggesting the importance of being included.

Regarding the NL fraction, differences were perceived depending on the considered group of algae. Within red macroalgae, DAG was the most abundant, ranging from 9.1% (shade-dried *A. taxiformis*) to 12.2% (sun-dried *A. armata*). On the other hand, in brown macroalgae, TAG was the main contribution for NL sum (from 11.3, in sun-dried *T. abies-marina* up to 23.8%, in shade-dried *C. humilis*). Although TAG was not detected in sun-dried *A. taxiformis*, it was present in shade-dried *A. taxiformis*. Nelson *et al.*[135] didn't detect TAG in red algae *Chondracanthus canaliculatus*. On the contrary, these authors detected values between 0.9, in winter, up to 22.0% in spring, in the brown macroalgae *Egregia menziesii*[135]. Thus, it is important to note that, since TAG is the most prevalent NL accumulated in algae as a storage product and energy reservoir, they are stored in cytosolic lipid bodies and reutilized for polar lipid synthesis in the dark[129]. Higher amounts of FFA were detected in brown macroalgae, namely in shade-dried *T. abies-marina*, reaching 17.1%.

In the end, it is worth explaining the reason why the results were expressed in percentages rather than in absolute content. At first, the results of selected macroalgae exhibited a great heterogenicity in the lipid classes identified, which was already expectable. As a result, some lipid classes were below the working range established in methods validation. To overcome this challenge, it would be necessary to increase the amount of sample that was applied. Nonetheless,

that would entail a more pronounced interference by pigments, that would compromise the rigorous assessment in those bands that usually get fixed nearby, as it happens with MGDG.

4.3. Macroalgae fatty acid profile

The FA profile of each macroalgae was determined and the results obtained, expressed in % of total FA and mg/100 g dw, are summarized in Table 4.5 and Table 4.6, respectively.

Table 4.5 Fatty acid profile of selected macroalgae for both drying conditions, expressed as % of total FA.

	A. armata		***A. taxiformis***		***C. humilis***		***T. abies-marina***	
	Sun-dried	Shade-dried	Sun-dried	Shade-dried	Sun-dried	Shade-dried	Sun-dried	Shade-dried
14:0	19.4 ± 0.1^{g}	13.6 ± 0.1^{d}	17.4 ± 0.3^{f}	15.3 ± 0.1^{e}	2.9 ± 0.0^{a}	3.3 ± 0.1^{a}	5.2 ± 0.0^{c}	4.0 ± 0.2^{b}
16:0	53.8 ± 0.5^{f}	49.6 ± 0.3^{d}	54.7 ± 0.0^{f}	51.6 ± 0.5^{e}	30.1 ± 0.1^{b}	28.3 ± 0.1^{a}	34.1 ± 0.3^{c}	27.5 ± 0.3^{a}
18:0	2.0 ± 0.0^{b}	2.0 ± 0.0^{b}	1.9 ± 0.0^{b}	2.3 ± 0.1^{c}	1.0 ± 0.0^{a}	1.1 ± 0.2^{a}	1.1 ± 0.0^{a}	0.9 ± 0.0^{a}
20:0	0.5 ± 0.0^{c}	0.3 ± 0.0^{a,b}	0.3 ± 0.0^{a}	0.3 ± 0.0^{b}	0.5 ± 0.0^{d}	0.4 ± 0.0^{c}	0.8 ± 0.0^{e}	0.5 ± 0.0^{d}
22:0	0.2 ± 0.0^{a}	0.3 ± 0.0^{b}	ND[1]	0.3 ± 0.0^{c}	0.5 ± 0.0^{e}	0.5 ± 0.0^{e}	ND	0.4 ± 0.0^{d}
∑ SFA	**80.4 ± 0.6^{h}**	**71.0 ± 0.4^{e}**	**79.1 ± 0.4^{g}**	**75.0 ± 0.6^{f}**	**38.4 ± 0.0^{c}**	**37.0 ± 0.3^{b}**	**42.9 ± 0.3^{d}**	**35.2 ± 0.5^{a}**
16:1 *n*-7	6.1 ± 0.1^{e}	3.2 ± 0.0^{d}	6.6 ± 0.1^{f}	6.1 ± 0.0^{e}	1.9 ± 0.1^{a,b}	1.8 ± 0.0^{a}	2.5 ± 0.0^{c}	2.1 ± 0.0^{b}
18:1 *n*-9	4.7 ± 0.1^{b}	9.5 ± 0.1^{c}	4.1 ± 0.0^{a}	4.0 ± 0.0^{a}	14.6 ± 0.1^{d}	14.7 ± 0.4^{d}	18.8 ± 0.1^{f}	15.7 ± 0.0^{e}
18:1 *n*-7	1.5 ± 0.0^{e}	2.1 ± 0.0^{f}	2.4 ± 0.0^{g}	2.1 ± 0.0^{f}	1.2 ± 0.0^{d}	0.8 ± 0.0^{c}	0.5 ± 0.0^{a}	0.7 ± 0.0^{b}
∑ MUFA	**14.4 ± 0.4^{a,b}**	**16.8 ± 0.2^{c}**	**14.8 ± 0.0^{b}**	**14.0 ± 0.1^{a}**	**18.9 ± 0.1^{d}**	**18.5 ± 0.4^{d}**	**22.7 ± 0.1^{f}**	**19.9 ± 0.0^{e}**
18:2 *n*-6	0.4 ± 0.0^{a}	1.0 ± 0.1^{b}	1.3 ± 0.0^{c}	1.4 ± 0.1^{c}	7.3 ± 0.0^{f}	7.3 ± 0.1^{f}	5.4 ± 0.0^{d}	6.0 ± 0.0^{e}
18:3 *n*-3	0.1 ± 0.0^{a}	0.6 ± 0.0^{b}	0.4 ± 0.0^{b}	0.4 ± 0.0^{b}	6.7 ± 0.0^{d}	7.2 ± 0.2^{e}	5.7 ± 0.0^{c}	8.3 ± 0.0^{f}
18:4 *n*-3	0.2 ± 0.0^{a}	1.8 ± 0.0^{c}	1.1 ± 0.1^{b}	1.1 ± 0.0^{b}	4.6 ± 0.0^{e}	5.1 ± 0.2^{f}	1.9 ± 0.0^{c}	3.3 ± 0.0^{d}
20:4 *n*-6	0.2 ± 0.0^{a}	2.8 ± 0.0^{c}	1.0 ± 0.0^{b}	0.9 ± 0.0^{b}	14.0 ± 0.1^{d}	14.3 ± 0.1^{d}	15.3 ± 0.2^{e}	17.4 ± 0.3^{f}
20:5 *n*-3	0.6 ± 0.0^{a}	2.9 ± 0.2^{b}	ND	2.9 ± 0.0^{b}	5.5 ± 0.0^{d}	6.3 ± 0.2^{e}	2.9 ± 0.0^{b}	4.9 ± 0.1^{c}
22:6 *n*-3	ND	ND	ND	0.2 ± 0.1^{a}	0.2 ± 0.0^{a}	0.5 ± 0.0^{b}	ND	ND
∑ PUFA	**5.2 ± 0.2^{a}**	**12.3 ± 0.2^{c}**	**6.1 ± 0.4^{a}**	**11.0 ± 0.5^{b}**	**42.7 ± 0.1^{e}**	**44.5 ± 0.7^{f}**	**34.4 ± 0.3^{d}**	**44.8 ± 0.5^{f}**
∑ *n*-3	1.8 ± 0.1^{a}	5.6 ± 0.2^{c}	1.8 ± 0.2^{a}	4.9 ± 0.1^{b}	19.0 ± 0.0^{f}	21.4 ± 0.6^{g}	11.7 ± 0.0^{d}	18.1 ± 0.1^{e}
∑ *n*-6	2.6 ± 0.3^{a}	6.1 ± 0.0^{d}	3.7 ± 0.2^{b}	5.3 ± 0.3^{c}	23.4 ± 0.1^{f}	22.7 ± 0.1^{e}	22.1 ± 0.3^{e}	26.2 ± 0.4^{g}
***n*-3/*n*-6**	0.7 ± 0.1^{b}	0.9 ± 0.0^{b,c}	0.5 ± 0.0^{a}	0.9 ± 0.0^{b,c}	0.8 ± 0.0^{b,c}	0.9 ± 0.0^{d}	0.5 ± 0.0^{a}	0.7 ± 0.0^{b}

Values are presented as average ± standard deviation. Different lowercase letters within a row correspond to significant statistical differences ($p < 0.05$).
[1]ND - not detected

Table 4.6 Fatty acid profile of selected macroalgae for both drying conditions, expressed in mg/100 g dw.

	A. armata		***A. taxiformis***		***C. humilis***		***T. abies-marina***	
	Sun-dried	Shade-dried	Sun-dried	Shade-dried	Sun-dried	Shade-dried	Sun-dried	Shade-dried
14:0	124.0 ± 9.2^{d}	98.2 ± 2.3^{c}	135.2 ± 2.6^{e}	92.5 ± 0.4^{c}	21.7 ±0.3^{a}	27.2 ± 0.3^{a,b}	33.0 ± 3.4^{b}	18.4 ± 1.3^{a}
16:0	344.1 ± 27.5^{c,d}	358.6 ± 7.6^{d}	424.1 ± 0.3^{e}	312.4 ± 0.2^{c}	223.4 ± 1.5^{b}	231.4 ± 2.9^{b}	218.3 ± 22.8^{b}	126.6 ± 4.2^{a}
18:0	12.8 ± 0.7^{d}	14.8 ± 0.1^{e}	14.5 ± 0.1^{e}	14.0 ± 0.2^{d,e}	7.3 ± 0.1^{b}	8.9 ± 1.2^{c}	6.8 ± 0.7^{b}	4.3 ± 0.1^{a}
20:0	2.9 ± 0.3^{b}	2.3 ± 0.0^{a}	2.3 ± 0.0^{a}	2.0 ± 0.0^{a}	3.6 ± 0.0^{c}	3.6 ± 0.1^{c}	4.9 ± 0.4^{d}	2.2 ± 0.0^{a}
22:0	1.1 ± 0.1^{a}	1.8 ± 0.0^{b,c}	ND[1]	2.0 ± 0.2^{c}	4.0 ± 0.0^{d}	4.3 ±0.1^{d}	ND	1.7 ± 0.0^{b}
∑ SFA	**514.1 ± 39.8^{d}**	**513.0 ± 10.2^{d}**	**613.3 ± 3.4^{e}**	**454.1 ± 1.5^{c}**	**284.4 ± 1.5^{b}**	**302.2 ± 2.6^{b}**	**275.2 ± 28.7^{b}**	**162.1 ± 5.7^{a}**
16:1 *n*-7	38.9 ± 1.8^{d}	23.0 ± 0.2^{c}	51.3 ± 0.6^{e}	37.2 ± 0.1^{d}	14.2 ± 0.7^{b}	14.7 ± 0.3^{b}	15.9 ± 1.6^{b}	9.5 ± 0.4^{a}
18:1 *n*-9	30.1 ± 1.5^{a}	68.7 ± 0.5^{b}	31.7 ± 0.1^{a}	24.3 ± 0.1^{a}	108.3 ± 0.5^{c}	120.4 ± 1.3^{d}	120.4 ± 11.0^{d}	72.1 ± 1.7^{b}
18:1 *n*-7	9.3 ± 0.5^{c}	15.3 ± 0.1^{e}	18.6 ± 0.4^{f}	13.0 ± 0.1^{d}	8.6 ± 0.1^{c}	6.6 ± 0.4^{b}	3.5 ± 0.3^{a}	3.2 ± 0.0^{a}
∑ MUFA	**91.9 ± 3.9^{a}**	**121.1 ± 0.6^{b}**	**114.8 ± 0.1^{b}**	**84.7 ± 1.3^{a}**	**140.1 ± 1.1^{c}**	**151.0 ± 1.1^{c}**	**145.0 ± 13.6^{c}**	**91.6 ± 2.1^{a}**
18:2 *n*-6	2.61 ± 0.18^{a}	7.5 ± 0.5^{b}	10.2 ± 0.1^{b}	8.7 ± 0.8^{b}	54.9 ± 0.2^{e}	59.6 ± 1.9^{f}	34.4 ± 3.3^{d}	27.6 ± 0.6^{c}
18:3 *n*-3	0.6 ± 0.1^{a}	4.2 ± 0.1^{a}	3.0 ± 0.1^{a}	2.6 ± 0.3^{a}	49.9 ± 0.1^{c}	59.1 ± 2.6^{d}	36.8 ± 3.6^{b}	38.0 ± 0.9^{b}
18:4 *n*-3	1.6 ± 0.1^{a}	12.8 ± 0.2^{c,d}	8.7 ± 0.8^{b}	6.5 ± 0.0^{b}	34.2 ± 0.3^{e}	41.3 ± 1.9^{f}	12.4 ± 1.3^{c}	15.3 ± 0.3^{d}
20:4 *n*-6	1.5 ± 0.0^{a}	20.5 ± 0.0^{b}	7.4 ± 0.0^{a}	5.7 ± 0.1^{a}	104.1 ± 0.2^{d}	116.8 ± 1.2^{e}	97.9 ± 8.1^{d}	79.9 ± 0.3^{c}
20:5 *n*-3	4.1 ± 0.6^{a}	20.8 ± 0.8^{c,d}	ND	17.3 ± 0.1^{b}	40.9 ± 0.2^{e}	51.3 ± 2.9^{f}	18.7 ± 1.6^{b,c}	22.7 ± 0.1^{d}
22:6 *n*-3	ND	ND	ND	1.2 ± 0.4^{a}	1.55 ± 0.03^{a}	4.2 ± 0.1^{b}	ND	ND
∑ PUFA	**33.1 ± 0.8^{a}**	**88.6 ± 0.4^{c}**	**46.9 ± 2.9^{a,b}**	**66.8 ± 3.8^{b,c}**	**316.6 ± 0.7^{e}**	**363.7 ± 12.0^{f}**	**220.0 ± 19.4^{d}**	**206.1 ± 2.2^{d}**
Total FA	**639.1 ± 44.5^{b}**	**722.6 ± 10.4^{c}**	**774.9 ± 0.5^{c,d}**	**605.6 ± 6.6^{b}**	**741.1 ± 3.3^{c,d}**	**816.9 ± 13.5^{d}**	**640.2 ± 61.7^{b}**	**459.8 ± 10.0^{a}**
∑ *n*-3	11.4 ± 1.3^{a}	40.6 ± 1.2^{b}	14.1 ± 1.5^{a}	29.6 ± 0.9^{b}	140.7 ± 0.7^{d}	174.8 ± 8.0^{e}	74.8 ± 7.2^{c}	83.3 ± 1.4^{c}
∑ *n*-6	16.4 ± 0.9^{a}	44.2 ± 0.6^{c}	28.5 ± 1.4^{a,b}	32.4 ± 2.1^{b,c}	173.3 ± 0.0^{f}	185.2 ± 3.9^{e}	141.2 ± 11.6^{e}	120.4 ± 0.7^{d}

Values are presented as average ± standard deviation. Different lowercase letters within a row correspond to significant statistical differences ($p < 0.05$).
[1]ND - not detected

The results presented in Table 4.5 highlight very different FA profiles between red (*A. taxiformis* and *A. armata*) and brown macroalgae (*C. humilis and T. abies-marina*). The highest SFA contents were determined in red macroalgae species, while PUFA were the most abundant among brown algae. The SFA varied from 35.2 to 80.4% of total FA, in shade-dried *T. abies-marina* and in sun-dried *A. armata*, respectively, which corresponded in the same order, to 162.1 and 514.1 mg/100 g dw. However, within the Rhodophyta and Phaeophyceae species, the found variability was much lower. The SFA content in the Rhodophyta ranged between 71.0 and 80.4% (in shade-dried *A. armata* and in sun-dried *A. armata*, respectively), while in Phaeophyceae it varied between 35.2 and 42.9% (in shade-dried *T. abies-marina* and in sun-dried *T. abies-marina*, respectively). The observed trend was also reported in other studies carried in other macroalgae, in which SFA were always the most abundant group of FA in Rhodophytes[25,116,136,137]. It was observed that among SFA, palmitic acid (16:0) was the FA with the highest contribution,

regardless of the macroalgae considered. Within red algae, this FA alone accounted for nearly half of total FA. In particular, sun-dried *A. taxiformis*, showed to have the highest relative contents of palmitic acid (54.7% of total FA, corresponding to 424.1 mg/100 g dw). Myristic acid (14:0) was the second most abundant SFA and, once more, with significantly higher contents in the studied red algae, where it corresponded up to 19.4% (sun-dried *A. armata*). In brown algae counterparts, the highest myristic acid content was observed in sun-dried *T. abies-marina* with 5.2%. This preponderance of both palmitic and myristic acids was also noticed by Regal *et al.*[40], in *A. taxiformis*, with relative contents similar to those found in this study (nearly 58% of total FA for palmitic and around 16% for myristic acid). Palmitic acid dominance, followed by myristic acid, was also reported in previous studies carried in both red and brown macroalgae[8,15,116,138].

Regarding PUFA, shade-dried *C. humilis* and *T. abies-marina* had the highest PUFA levels. For these macroalgae PUFA corresponded up to almost 45% of total FA. These relative contents, however, were lower in sun-dried macroalgae, particularly in *T. abies-marina* where PUFA corresponded to 34.4%, which is nearly 10% less than the shade-dried algae. Nevertheless, these results follow the same distribution as referred by Wielgosz-Collin *et al.*[27], where PUFA and SFA represent 80% of total FA in brown macroalgae species. Within *C. humilis* macroalgae, PUFA absolute content corresponded to 316.6 and 363.7 mg/100 g dw in sun- and shade-dried biomass, respectively. In turn, in sun- and shade-dried *T. abies-marina*, the levels of PUFA absolute content found were 220.0 and 206.1 mg/100 g dw, respectively. These results were leveraged by the levels of arachidonic acid (ARA, 20:4 *n*-6). The ARA relative contents varied from 14.0 up to 17.4% (sun-dried *C. humilis* and shade-dried *T. abies-marina*, respectively). The absolute content of ARA, in *C. humilis*, corresponded to 104.1 and 116.8 mg/100 g dw (sun- and shade-dried, by the same order), while in *T. abies-marina* it accounted for 97.9 and 79.9 mg/100 g dw (sun- and shade-dried, respectively). Similar results were also observed by Vizetto-Duarte *et al.*[48], that reported ARA as the main PUFA, in other *Cystoseira* species: *C. compressa* (20.1%), *C. tamariscifolia* (22.8%), *C. nodicaulis* (26.5%), *C. baccata* (19.9%) and *C. barbata* (19.1%). These authors also found ARA in *C. humilis* (11.7%), however, in their study linoleic acid (LA, 18:2 *n*-6) was the most abundant PUFA (17.1%).

Even though the importance of dietary intake of *n*-3 PUFA has been extensively studied, much less effort has been made regarding *n*-6 PUFA like ARA. Due to its pro-inflammatory effect, for example, ARA have been frequently related to a negative connotation[139]. However, recent studies have pointed out this FA as an integral constituent of the biological cell membranes, being required for cells functioning, namely in the nervous system, skeletal muscle, and immune system[140]. Thus, it has been recognised as useful in developing the immune response, thrombosis and brain function, as well as in the neurological development of the infants, where it plays an important role in the structure of neurons, in the central nervous system[140–143]. Having in mind

that inflammation is an essential defence mechanism, responsible for combating antigens, restoring homeostasis, and repairing tissue damage, the eicosanoids, including the ones derived from ARA, have been pinpointed with central roles in the regulation of tissue repair and wound healing[144,145]. As ARA drives inflammatory response to strength training, recently, Souza *et al.*[146] and Mitchell *et al.*[147] established a positive correlation between ARA supplementation and strength training induced adaptations. In fact, ARA levels that were found in this study are comparable or even higher to those found in other foods, including meats and poultry (24 – 104 mg/100 g of edible portion), which are considered as good sources of this FA[148]. Furthermore, the macroalgae studied have a much lower fat content when compared to these foods. Besides, ARA also seems to be beneficial for aquaculture where it is involved in fish stress response[149,150]. Other studies have also shown that that increasing dietary ARA improved the growth of several fish species[151]. This means that the studied macroalgae may also find applications in aquafeeds.

Among the n3-PUFA, linolenic acid (ALA, 18:3 *n*-3), stearidonic acid (SDA, 18:4 *n*-3), and eicosapentaenoic acid (EPA, 20:5 *n*-3) were also found in brown macroalgae, although at less amounts, when compared to ARA. In global terms, the levels of these FA never reached 9% of total FA. DHA was detected but only at trace levels, which seems to be characteristic from brown macroalgae[27,48,137]. In what concerns red algae, the relative amounts of PUFA recorded never surpassed 13.0% and were even lower in sun-dried samples. While shade-dried red algae presented 12.3 and 11.0% (found in *A. armata* and *A. taxiformis*, in the same order), the sun-dried counterparts only had 6.1 and 5.2% (*A. taxiformis* and *A. armata*, respectively). The EPA was the most abundant PUFA, with 2.9% of total FA, in both shade-dried *Asparagopsis*, representing 20.8 and 17.3 mg/100 g dw, in shade-dried *A. armata* and shade-dried *A. taxiformis*, respectively. A similar relative content of EPA in *A. armata*, was also found by Pereira *et al.*[137]. The found EPA content was quite low when compared to other red algae, which are commonly reported as good EPA sources[89,136,137,152,153]. It should be pointed out that EPA content in *A. taxiformis* and *A. armata* macroalgae was significantly affected by sun-drying.

MUFA were equally distributed among the analysed macroalgae, showing lower variability, when compared to SFA and PUFA, and ranged from 14.0% of total FA (corresponding to 84.7 mg/100 g dw), in shade-dried *A. taxiformis*, to 22.7% of total FA (corresponding to 145.0 mg/100 g dw), in sun-dried *T. abies-marina*. In red macroalgae both oleic (18:1 *n*-9) and palmitoleic (16:1 *n*-7) acids stood out as the main MUFA, whereas, in brown macroalgae, oleic acid was preponderant when compared with palmitoleic values. Wielgosz-Collin *et al.*[27] referred to these two FA as the main MUFA found in both brown macroalgae. Also, Pereira *et al.*[137] found similar results in brown macroalgae, including *S. vulgare*, *Halopteris scoparia*, *Dictyota dichotoma* and *D. spiralis*, and in red macroalgae, including *A. armata*, *Pterocladiella capillacea*, *Peyssonnelia* sp. and *Bornetia secundiflora*: the dominance of both oleic and palmitoleic in MUFA. However, in

the present study, brown macroalgae showed more abundance of oleic acid, when compared with red macroalgae. Oleic acid highest content was observed in *T. abies-marina* sun-dried (18.8% of total FA, corresponding to 120.4 mg/100 g dw), while the highest palmitoleic acid content was found in *A. taxiformis* sun-dried (6.6% of total FA, which corresponded to 51.3 mg/100 g dw).

In what concerns global FA of *A. armata* determined in this study, it was also similar to the one observed by Pereira *et al.*[137], in macroalgae harvested in Algarve coastal beaches, including the proportion of SFA, MUFA, and PUFA, as well as the predominance of palmitic acid over other FA. It is also worth mentioning, that the FA acid profiles found in *T. abies-marina* were similar to the profile reported by Fonseca *et al.*[154], that studied the same macroalgae harvested, also in Faial island in June 2019.

The studied macroalgae had a balanced *n*-3/*n*-6 ratio, up to 0.9, thus not exceeding the proportion of 1:10, as recommended by the World Health Organization[27].

Lipids oxidation is highly dependent on environmental conditions after algae harvesting. High temperatures, light exposure, the composition of sample matrix, the FA profile, or the drying process, are some factors that may affect the oxidation extend. There are several studies concerning the impact of the drying process in FA oxidation. Chan *et al.*[155], for example, found that *S. hemiphyllum* nutritional composition was greatly affected by different drying processes, being total PUFA content higher in freeze-dried than in oven-dried samples. Regal *et al.*[40] also included the drying process as one of the causes for changes in biochemical composition and bioactivity, in *A. taxiformis*. Furthermore, PUFA are known to be susceptible to light-induced photooxidation[158,159]. The FA oxidation rate increases exponentially with the unsaturation degree. For example, 18:3 has a 2500-fold faster oxidation rate than the saturated 18:0[160]. For these reasons, it was expected that shade-dried samples, could have higher PUFA amounts than samples dried in sunlight, as this drying process may result in lipid deterioration (with the concomitant increase in SFA). This hypothesis was fully confirmed by the results shown in Table 4.6, once the SFA levels were significantly higher in sun-dried samples when comparing to shade-dried ones, namely, in *A. armata, A. taxiformis,* and *T. abies-marina*. Among the studied macroalgae, *C. humilis*, was the exception, in which the differences in SFA levels, resulting from distinct drying processes were less pronounced. In this regard, brown macroalgae are known to contain important contents of antioxidants and polyphenols that may have prevented the accumulation of SFA. In particular, when compared to *T. abies-marina*, *C. humilis* showed higher polyphenol contents and a higher antioxidant activity (data not published yet), which might have contributed to the lower SFA accumulation in the latter.

4.4. Fatty acid profile of polar lipid classes

Among the four macroalgae included in this study, *C. humilis* and *T. abies-marina*, had the most intense and the best-defined GL bands, when compared to red macroalgae. For these reasons, only these two macroalgae were evaluated in terms of their PL classes FA profile. Furthermore, sun-drying was the selected processing condition. The results obtained are summarized in Table 4.7.

Table 4.7 Fatty acid profile of *C. humilis* and *T. abies-marina* polar lipid classes, expressed in % of total FA.

	C. humilis				***T. abies-marina***			
	PC	**PE+SQDG**	**DGDG**	**MGDG**	**PC**	**PE+SQDG**	**DGDG**	**MGDG**
14:0	2.1 ± 0.4^{a}	2.2 ± 0.0^{a}	2.7 ± 0.4^{a}	4.0 ± 0.0^{c,d}	2.4 ± 0.1^{a}	3.9 ± 0.0^{b}	4.5 ± 0.1^{d}	5.7 ± 0.2^{e}
16:0	26.3 ± 0.6^{b}	48.1 ± 0.5^{e}	27.0 ± 0.8^{b}	29.0 ± 0.2^{c}	18.8 ± 0.5^{a}	52.4 ± 0.2^{f}	34.1 ± 0.8^{e}	30.6 ± 0.0^{d}
18:0	3.2 ± 0.1^{f}	0.8 ± 0.0^{a}	1.2 ± 0.1^{b}	1.7 ± 0.0^{d}	1.9 ± 0.1^{e}	0.8 ± 0.0^{a}	1.2 ± 0.0^{b}	1.4 ± 0.0^{c}
20:0	ND[1]	0.4 ± 0.0^{a}	0.6 ± 0.1^{c}	0.5 ± 0.0^{b}	1.0 ± 0.0^{f}	0.8 ± 0.0^{d}	0.8 ± 0.0^{d}	0.9 ± 0.0^{e}
∑ SFA	**33.6 ± 0.7^{b}**	**52.7 ± 0.5^{e}**	**34.2 ± 1.0^{b}**	**38.6 ± 0.3^{c}**	**26.7 ± 0.4^{a}**	**60.7 ± 0.1^{f}**	**42.6 ± 0.9^{d}**	**41.4 ± 0.3^{d}**
16:1 *n*-7	ND	1.6 ± 0.0^{a}	1.6 ± 0.1^{a}	1.7 ± 0.0^{a}	2.7 ± 0.0^{d}	2.1 ± 0.0^{b}	2.5 ± 0.1^{c}	2.4 ± 0.0^{c}
18:1 *n*-9	11.0 ± 0.1^{a}	22.9 ± 0.0^{e}	14.5 ± 0.5^{c}	12.9 ± 0.1^{b}	15.1 ± 0.2^{c}	23.6 ± 0.2^{e}	17.8 ± 0.3^{d}	14.8 ± 0.2^{c}
18:1 *n*-7	6.0 ± 0.1^{f}	1.1 ± 0.0^{d}	0.8 ± 0.0^{b,c}	0.9 ± 0.0^{c,d}	2.1 ± 0.2^{e}	1.0 ± 0.0^{c,d}	0.6 ± 0.0^{b}	0.3 ± 0.0^{a}
∑ MUFA	**16.9 ± 0.2^{b}**	**25.8 ± 0.0^{e}**	**17.7 ± 0.4^{c}**	**16.0 ± 0.2^{a}**	**20.6 ± 0.3^{d}**	**27.3 ± 0.2^{f}**	**21.7 ± 0.3^{e}**	**18.5 ± 0.2^{c}**
18:2 *n*-6	5.7 ± 0.1^{c}	4.1 ± 0.1^{a}	10.4 ± 0.4^{e}	6.7 ± 0.1^{d}	5.5 ± 0.1^{b,c}	ND	5.2 ± 0.1^{b}	5.4 ± 0.1^{b,c}
18:3 *n*-3	2.9 ± 0.1^{b}	4.1 ± 0.1^{c}	8.3 ± 0.2^{f}	5.3 ± 0.1^{d}	3.0 ± 0.1^{b}	2.4 ± 0.0^{a}	5.8 ± 0.1^{e}	5.6 ± 0.1^{d,e}
18:4 *n*-3	2.1 ± 0.1^{d}	0.6 ± 0.0^{b}	8.4 ± 0.1^{g}	4.0 ± 0.1^{f}	0.9 ± 0.0^{c}	0.2 ± 0.0^{a}	2.4 ± 0.0^{e}	2.2 ± 0.0^{d,e}
20:4 *n*-6	20.8 ± 1.0^{f}	6.1 ± 0.3^{b}	8.0 ± 0.4^{c}	12.1 ± 0.2^{d}	24.9 ± 0.5^{g}	3.6 ± 0.1^{a}	11.9 ± 0.1^{d}	14.5 ± 0.3^{e}
20:5 *n*-3	5.9 ± 0.2^{e}	1.3 ± 0.1^{b}	10.1 ± 0.5^{f}	3.9 ± 0.1^{d}	4.2 ± 0.1^{d}	0.4 ± 0.0^{a}	2.7 ± 0.0^{c}	2.7 ± 0.1^{c}
22:6 *n*-3	ND	ND	ND	ND	ND	ND	ND	ND
∑ PUFA	**40.7 ± 1.6^{e}**	**17.7 ± 0.7^{b}**	**46.0 ± 1.7^{f}**	**35.2 ± 0.6^{d}**	**43.5 ± 0.9^{f}**	**7.4 ± 0.1^{a}**	**30.5 ± 0.3^{c}**	**32.5 ± 0.5^{c,d}**
∑ *n*-3	12.3 ± 0.5^{d}	6.2 ± 0.3^{b}	27.5 ± 0.8^{f}	14.5 ± 0.3^{e}	10.0 ± 0.3^{c}	4.2 ± 0.0^{a}	11.5 ± 0.2^{d}	11.6 ± 0.2^{d}
∑ *n*-6	28.4 ± 1.2^{e}	10.4 ± 0.4^{b}	18.4 ± 0.8^{c}	20.2 ± 0.3^{d}	32.5 ± 0.6^{f}	3.8 ± 0.1^{a}	18.6 ± 0.3^{c}	20.5 ± 0.3^{d}

Values are presented as average ± standard deviation. Different lowercase letters within a row correspond to significant statistical differences ($p < 0.05$).
[1]ND - not detected

In global terms, the results regarding the FA of the PL classes that were obtained in this work reflect the FA composition that was observed for other brown algae[52,132]. The results highlight that the distribution of PUFA among the PL classes follows the trend: DGDG > PC > MGDG > PE+SQDG, for *C. humilis* and PC > MGDG > DGDG > PE+SQDG for *T. abies-marina*. In the brown algae *L. japonica*, Sanina and co-workers[132] found the following trend for PUFA

distribution among PL classes: MGDG > PC > PE > DGDG > SQDG. High amounts of PUFA were found in PC, as well as in the MGDG fraction. The content of PUFA found in the PC fraction corresponded to 40.7 and 43.5% of total FA, determined in *C. humilis* and *T. abies-marina*, respectively. In what concerns the MGDG fraction, PUFA accounted for 35.2 and 32.5% of total FA (by the same order in *C. humilis* and *T. abies-marina*). The PUFA relative contents were leveraged by ARA, that was the most abundant FA in PC fraction, representing 20.8 and 24.9% of total FA (*C. humilis* and *T. abies-marina*, respectively). In this regard, it should be mentioned that Sanina *et al.*[132] have also observed in *L. japonica* a relevant contribution of ARA for the PC fraction of the FA profile. These authors reported that ARA represented 29.1% of PC fraction total FA. High relative contents of ARA were also found in MGDG, namely in *T. abies-marina*, where this FA represented 14.5% of total FA. The prevalence of ARA over EPA in most PL classes, suggests that the former FA may be more functionally important[132]. PUFA, namely ARA, preferential location in PC is of great importance since it was reported that FA included in the phospholipids fractions showed higher bioaccessibility in comparison, for instance, with MAG or TAG[161,162]. The ARA abundance in brown macroalgae might suggest that this FA plays a role as an eicosanoid precursor, as observed in animals. According to Sanina *et al.*[132], this is a plausible hypothesis when very low percentage of LA and ALA occur. However, in opposition to the observations by these authors EPA contents recorded were always low: both in PL fractions and on the whole freeze-dried macroalgae. It was also found, in PC, that EPA contribution ranged from 5.9 and 4.2% of total FA (in C. *humilis* and *T. abies-marina*, respectively). Furthermore, within GL, results also highlight that PUFA were also present in substantial amounts in DGDG fractions (corresponding to nearly 30.5 and 46% of total FA, in *T. abies-marina* and *C. humilis*, respectively), similarly to what was denoted by other authors in their studies with brown macroalgae[52,132]. In both *C. humilis* and *T. abies-marina*, LA and ALA were mostly present in MGDG. In view of this, it can be hypothesised that the high PUFA contents found in MGDG and DGDG fractions may reflect their higher contribute to the photosynthetic function of studied algae[143].

Just as observed in other brown macroalgae species, PE+SQDG was the most saturated lipid class[52,132,163]. For this fraction, SFA represented 52.7 and 60.7% of total FA, in *C. humilis* and *T. abies-marina*, respectively, with palmitic acid being the most prevalent. Indeed, this FA corresponded to nearly half of total FA identified in PE+SQDG fraction: 48.1 and 52.4% determined, by the same order, in *C. humilis* and *T. abies-marina*. These observations are consistent with other studies that have identified palmitic acid as the main FA in SQDG fractions from marine algae[52,132,164]. Plouguerné *et al.*[69] have proposed that palmitic acid may play an important role in SQDG antiviral activity. This may be of great interest in future studies, where the antiviral potential of these macroalgae can be checked as a way to upgrade these species.

Regarding MUFA, it was observed that the highest relative contents were found in both PE+SQDG fractions from *T. abies-marina* (27.3% of total FA) and *C. humilis* (25.8% of total FA). Oleic acid was globally the main MUFA among all PL groups: representing from 11 to 23.6% of total FA, in PC from *C. humilis*, and in PE+SQDG from *T. abies-marina*, respectively.

5. Conclusions and future prospects

Marine organisms represent nearly half of worldwide biodiversity, in which macroalgae stand out as a vast source of natural bioactive compounds. The range of beneficial biological activities identified so far has led to a higher demand for the use of macroalgae in a wide variety of applications. Among the bioactive compounds with interest, lipids are important constituents of these organisms. Within its lipid fraction, PL are often the main lipid class in macroalgae, in which GL play key roles and have been associated with important beneficial health effects, such as antibacterial, antifungal, antioxidative, anti-inflammatory, and antitumor. Considering the bioactive potential of this group of lipids, an analytical protocol using an HPTLC system was optimized and validated for macroalgal lipid classes separation. Moreover, the lipid fraction of two red macroalgae, *A. armata* and *A. taxiformis*, along with two brown macroalgae, *C. humilis* and *T. abies-marina* were characterized in terms of TL content, lipid classes, and fatty acid profile.

Considering the analytical method used for lipid classes quantification using an HPTLC system, it was optimized and validated in terms of specificity, working range, analytical limits, and precision, for lipid classes using, namely, PC, SQDG, DGDG, SL, MGDG, DAG, FFA, and TAG. Regarding the lipid extraction, the best results were delivered by the Bligh and Dyer method, once it proved to be the most efficient regarding PL and GL extraction. The TL content recorded was similar among the four studied macroalgae species. In global terms, TL did not show significant differences between the selected macroalgae species. However, under certain circumstances, the drying process may interfere with TL quantification.

In what concerns to the lipid classes, *Asparagopsis* showed the highest PL levels. Within PL, MGDG was consistently the most abundant, while DGDG and SQDG were determined in lower amounts. In opposition to what was observed in red counterparts, the brown macroalgae exhibited higher levels of NL, representing nearly half of TL, in which TAG had the main contribution. A similar FA profile was detected for the different macroalgae: the main PUFA contribution was found in the brown macroalgae (*C. humilis* and *T. abies-marina*), in which ARA was predominant. In opposition to red macroalgae (*A. armata* and A. *taxiformis*), that showed the dominance of the SFA. In this study, shade-dried macroalgae showed higher levels of PUFA, when compared to sun-dried ones, allowing to conclude that the drying procedures can greatly affect the FA profile. Regarding the PL classes FA profile, it was observed that ARA was the predominant FA in phospholipids and MGDG, of both *C. humilis* and *T. abies-marina*. Indeed, these lipid classes were the ones with the highest PUFA contribution. It is also important to note that the highest ARA amounts in phospholipids fraction may render higher bioaccessibility of this FA. Considering ARA bioactivities, the found results are an important asset in what concerns to

these macroalgae upgrading, as a reliable source for this compound for a range of applications. From the commercial standpoint, along with the fact that these algae originated from pristine waters, the shade-drying process will contribute to product upgrading. Aquatic biomass, including macroalgae, are much more photosynthetic efficient than terrestrial plants. Besides, as CO_2 acquisition by marine macroalgae play an important role in carbon sequestration and improvement of greenhouse gas emissions, these organisms represent a sustainable source of bioactive compounds.

The results obtained in this study, allowed to highlight an upgrading potential, based on sustainable exploitation, that meets the Sustainable Development Goals as proposed by UN[165], namely:

- Goals 2 and 3: contributing to end hunger, ensuring healthy lives and promote well-being for all at all ages, making use of the biologically active molecules naturally present in macroalgae.
- Goal 13: take urgent action to combat climate change and its impacts: photosynthesis carried by macroalgae positively contributes to reducing the atmospheric CO_2 and greenhouse effect.
- Goal 14: conserve and sustainably use the oceans, seas, and marine resources for sustainable development: promoting the exploitation of endogenous algae, to prevent invasive species growth, thus preserving the biodiversity of the marine ecosystem.

Future work should include, for instance, the identification of other lipid classes, namely betaine lipids, as well as other phospholipids that were not included in this study but are known to be present in marine macroalgae. This could be accomplished using the same HPTLC system, but with other mobile phases and derivatization reagents, that could allow maximizing these compounds separation and quantification. Further experiments regarding the pigments should be undertaken to minimize their interference without compromising the lipids extraction efficiency. In the same way, the fractionation of the PL classes through PTLC should be optimized so it could allow a better separation of those bands that co-elute (PE+SQDG). Besides, the evaluation of seasonal changes in both TL content and PL and GL amounts in both red and brown macroalgae should also be taken into consideration, to accomplish a detailed characterization of their polar fraction.

6. References

1. Kiuru P, D'Auria MV, Muller C, Tammela P, Vuorela H, Yli-Kauhaluoma J. Exploring marine resources for bioactive compounds. *Planta Med*. 2014;80(14):1234-1246. doi:10.1055/s-0034-1383001

2. Hamed I, Ozogul Y, Regenstein JM. Marine bioactive compounds and their health benefits: a review. *Compr Rev Food Sci Food Saf*. 2015;14(4):446-465. doi:10.1111/1541-4337.12136

3. Zhao C, Yang C, Liu B, et al. Bioactive compounds from marine macroalgae and their hypoglycemic benefits. *Trends Food Sci Technol*. 2018;72:1-12. doi:10.1016/j.tifs.2017.12.001

4. MacArtain P, Gill CIR, Brooks M, Campbell R, Rowland IR. Nutritional value of edible seaweeds. *Nutr Rev*. 2007;65(12):535-543. doi:10.1301/nr.2007.dec.535

5. Cherry P, O'Hara C, Magee PJ, Mcsorley EM, Allsopp PJ. Risks and benefits of consuming edible seaweeds. *Nutr Rev*. 2019;77(5):307-329. doi:10.1093/nutrit/nuy066

6. Ragonese C, Tedone L, Beccaria M, et al. Characterisation of lipid fraction of marine macroalgae by means of chromatography techniques coupled to mass spectrometry. *Food Chem*. 2014;145:932-940. doi:10.1016/j.foodchem.2013.08.130

7. Melo T, Alves E, Azevedo V, et al. Lipidomics as a new approach for the bioprospecting of marine macroalgae — unraveling the polar lipid and fatty acid composition of *Chondrus crispus*. *Algal Res*. 2015;8:181-191. doi:10.1016/j.algal.2015.02.016

8. Kumar CS, Ganesan P, Pv S, Bhaskar N. Seaweeds as a source of nutritionally beneficial compounds – A review. *J Food Sci Technol*. 2008;45(1):1-13. doi:10.1002/9780470385869.ch26

9. Hamid N, Ma Q, Boulom S, et al. Chapter 8: Seaweed minor constituents. In: *Seaweed Sustainability*. Elsevier Inc.; 2015:193-242. doi:10.1016/B978-0-12-418697-2/00008-8

10. Khan W, Rayirath U, Subramanian S, et al. Seaweed extracts as biostimulants of plant growth and development. *J Plant Growth Regul*. 2009;28(4):386-399. doi:10.1007/s00344-009-9103-x

11. Cardoso SM, Carvalho LG, Silva PJ, Rodrigues MS, Pereira OR, Pereira L. Bioproducts from seaweeds: a review with special focus on the Iberian Peninsula. *Curr Org Chem*. 2014;18(7):896-917. doi:10.2174/1385272818071405151541116

12. Borowitzka MA. Algae as food. In: B.J.B. W, ed. *Microbiology of Fermented Foods*. Springer, Boston, MA; 1998. doi:10.1007/978-1-4613-0309-1_18

13. Pereira L. *As Algas Marinhas e Respectivas Utilidades*.; 2008.

14. Thomas N, Kim S. Potential pharmacological applications of polyphenolic derivatives from marine brown algae. *Environ Toxicol Pharmacol*. 2011;32(3):325-335. doi:10.1016/j.etap.2011.09.004

15. Mellouk Z, Benammar I, Krouf D, Goudjil M, Okbi M, Malaisse W. Antioxidant properties of the red alga *Asparagopsis taxiformis* collected on the North West Algerian coast. *Exp Ther Med*. 2017;13(6):3281-3290. doi:10.3892/etm.2017.4413

16. Duarte A. Optimization of seedling production using vegetative gametophytes of *Alaria esculenta*. 2017.

17. Jones CS, Mayfield SP. Algae biofuels: versatility for the future of bioenergy. *Curr Opin Biotechnol*. 2012;23(3):346-351. doi:10.1016/j.copbio.2011.10.013

18. Roberts T, Upham P. Prospects for the use of macro-algae for fuel in Ireland and the UK: an overview of marine management issues. *Mar Policy*. 2012;36(5):1047-1053. doi:10.1016/j.marpol.2012.03.001

19. Abomohra AE, El-naggar AH, Baeshen AA. Potential of macroalgae for biodiesel production: screening and evaluation studies. *J Biosci Bioeng*. 2017;125(2):231-237.

doi:10.1016/j.jbiosc.2017.08.020

20. Pimentel FB, Alves RC. Macroalgae-derived ingredients for cosmetic industry — an update. *cosmetics*. 2018;5(2):2-18. doi:10.3390/cosmetics5010002

21. Pereira L, Critchley AT. The COVID-19 novel coronavirus pandemic 2020: seaweeds to the rescue? Why does substantial, supporting research about the antiviral properties of seaweed polysaccharides seem to go unrecognized by the pharmaceutical community in these desperate times? *J Appl Phycol*. 2020;32:1875-1877. doi:10.1007/s10811-020-02143-y

22. Ahmed SA, Abdelrheem DA, El-mageed HRA, et al. Destabilizing the structural integrity of COVID-19 by caulerpin and its derivatives along with some antiviral drugs: an *in silico* approaches for a combination therapy. *Struct Chem*. 2020;31:2391–2412. doi:10.1007/s11224-020-01586-w

23. Morokutti-kurz M, König-schuster M, Koller C, et al. The intranasal application of zanamivir and carrageenan is synergistically active against Influenza A Virus in the murine model. *PLOS*. 2015;10(6):1-16. doi:10.1371/journal.pone.0128794

24. Gentile D, Patamia V, Scala A, Sciortino MT, Piperno A, Rescifina A. Putative inhibitors of SARS-CoV-2 main protease from a library of marine natural products: a virtual screening and molecular modeling study. *Mar Drugs*. 2020;18(4):2-19. doi:10.3390/md18040225.

25. Kumari P, Reddy CR., Jha B. Comparative evaluation and selection of a method for lipid and fatty acid extraction from macroalgae. *Anal Biochem*. 2011;415(2):134-144. doi:10.1016/j.ab.2011.04.010

26. Burtin P. Nutritional value of seaweeds. *Electron J Environ Agric Food Chem*. 2003;2(4):498-503.

27. Wielgosz-Collin G, Kendel M, Couzinet-Mossion A. Chapter 7: Lipids, fatty acids, glycolipids, and phospholipids. In: *Seaweed in Health Aand Disease Prevention*. Elsevier Inc.; 2016:185-221. doi:10.1016/B978-0-12-802772-1.00007-5

28. Lopes Í. Lipid profile and lipogenic capacity of the seaweed *Ulva lactuca* (Chlorophyta). Use as potential ingredient for fish aquaculture. 2016.

29. Kim S, Liu K, Lee S, et al. Effects of light intensity and nitrogen starvation on glycerolipid, glycerophospholipid, and carotenoid composition in *Dunaliella tertiolecta* culture. *PLoS One*. 2013;8(9):1-13. doi:10.1371/journal.pone.0072415

30. Misurcová L, Ambrozová J, Samek D. Chapter 27: Seaweed lipids as nutraceuticals. In: *Advances in Food and Nutrition Research*. Vol 64. ; 2011:339-355. doi:10.1016/B978-0-12-387669-0.00027-2

31. Costa E, Domingues P, Melo T, et al. Lipidomic signatures reveal seasonal shifts on the relative abundance of high-valued lipids from the brown algae *Fucus vesiculosus*. *Mar Drugs*. 2019;17(335):1-23. doi:10.3390/md17060335

32. Marinho GS, Holdt SL, Jacobsen C, Angelidaki I. Lipids and composition of fatty acids of *Saccharina latissima* cultivated year-round in integrated multi-trophic aquaculture. *Mar Drugs*. 2015;13(7):4357-4374. doi:10.3390/md13074357

33. Du Z, Benning C. Chapter 8: Triacylglycerol accumulation in photosynthetic cells in plants and algae. In: Nakamura Y, Li-Beisson Y, eds. *Lipids in Plant and Algae Development*. Springer International Publishing Switzerland 2016; 2016:179-205. doi:10.1007/978-3-319-25979-6

34. Gurgel C, Lopez-Bautista J. *Red Algae*.; 2007. doi:10.1002/9780470015902.a0000335

35. Cian R, Drago S, Medina F, Martínez-Augustin O. Proteins and carbohydrates from red seaweeds: evidence for beneficial effects on gut function and microbiota. *Mar Drugs*. 2015;13(8):5358-5383. doi:10.3390/md13085358

36. Usov AI. Polysaccharides of the red algae. *Adv Carbohydr Chem Biochem*. 2011;65:115-217. doi:10.1016/B978-0-12-385520-6.00004-2

37. Máximo P, Ferreira L, Branco P, Lima P, Lourenço A. Secondary metabolites and biological activity of invasive macroalgae of Southern Europe. *Mar Drugs*. 2018;16(265):1-28.

doi:10.3390/md16080265

38. Dijoux L, Viard F, Payri C. The more we search, the more we find: discovery of a new lineage and a new species complex in the genus *Asparagopsis*. *PLoS One*. 2014;9(7):1-13. doi:10.1371/journal.pone.0103826

39. Haslin C, Lahaye M, Pellegrini M, Chermann J. *In vitro* anti-HIV activity of sulfated cell-wall polysaccharides from gametic, carposporic and tetrasporic stages of the Mediterranean red alga *Asparagopsis armata*. *Planta Med*. 2001;67(4):301-305. doi:10.1055/s-2001-14330

40. Regal AL, Alves V, Gomes R, et al. Drying process, storage conditions, and time alter the biochemical composition and bioactivity of the anti-greenhouse seaweed *Asparagopsis taxiformis*. *Eur Food Res Technol*. 2020;246:781-793. doi:10.1007/s00217-020-03445-8

41. Cardigos F, Tempera F, Ávila S, Gonçalves J, Colaço A, Santos RS. Non-indigenous marine species of the Azores. *Helgol Mar Res*. 2006;60(2):160-169. doi:10.1007/s10152-006-0034-7

42. Roque BM, Salwen JK, Kinley R, Kebreab E. Inclusion of *Asparagopsis armata* in lactating dairy cows' diet reduces enteric methane emission by over 50 percent. *J Clean Prod*. 2019;234:132-138. doi:10.1016/j.jclepro.2019.06.193

43. Wehr JD. Brown Algae. In: *Freshwater Algae of North America*. Elsevier Inc.; 2015:851-871. doi:10.1016/B978-0-12-385876-4.00019-0

44. Montero L, Herrero M, Ibáñez E, Cifuentes A. Separation and characterization of phlorotannins from brown algae *Cystoseira abies-marina* by comprehensive two-dimensional liquid chromatography. *Eletrophoresis*. 2014;35(11):1-27. doi:10.1002/elps.201400133

45. Comission EU. ROC-POP-LIFE - Promoting biodiversity enhancement by restoration of Cystoseira populations. https://ec.europa.eu/environment/life/project/Projects/index.cfm?fuseaction=search.dspPage&n_proj_id=6334. Published 2017. Accessed June 4, 2020.

46. Grozdanić N, Kosanić M, Etahiri S, Assobhei O. An insight into cytotoxic and antimicrobial effects of *Cystoseira humilis* crude extract. *Stud Mar*. 2016;29(1):21-30.

47. Belattmania Z, Engelen AH, Pereira H, Serrão EA, Barakate M. Potential uses of the brown seaweed Cystoseira humilis biomass: 2- Fatty acid composition, antioxidant and antibacterial activities. *J Mater Environ Sci*. 2016;7(6):2074-2081.

48. Vizetto-duarte C, Pereira H, Sousa C, et al. Fatty acid profile of different species of algae of the *Cystoseira* genus: a nutraceutical perspective. *Nat Prod Res*. 2015;29(13):1264-1270. doi:10.1080/14786419.2014.992343

49. Barreto M, Mendonça E, Gouveia V, Anjos C, Medeiros J., Seca A. Macroalgae from S . Miguel island as a potential source of antiproliferative and antioxidant products. *Arquipelago Life Mar Sci*. 2012;29:53-58.

50. Mendis E, Kim S. Chapter 1: Present and future prospects of seaweeds in developing functional foods. In: *Advances in Food and Nutrition Research*. Vol 64. Elsevier Inc.; 2011:1-15. doi:10.1016/B978-0-12-387669-0.00001-6

51. Ferreira I, Gomes-Bispo A, Lourenço H, et al. The chemical composition and lipid profile of the chub mackerel (*Scomber colias*) show a strong seasonal dependence: contribution to a nutritional evaluation. *Biochimie*. 2020;178:181-189. doi:10.1016/j.biochi.2020.09.022

52. Khotimchenko S V, Division F. Distribution of glyceroglycolipids in marine algae and grasses. *Chem Nat Compd*. 2002;38(3):186-191.

53. Fahy E, Cotter D, Sud M, Subramaniam S. Lipid classification, structures and tools. *Biochim Biophys Acta*. 2011;1811:637-647. doi:10.1016/j.bbalip.2011.06.009

54. Li-beisson Y, Thelen JJ, Fedosejevs E, Harwood JL. The lipid biochemistry of eukaryotic algae. *Prog Lipid Res*. 2019;74:31-68. doi:10.1016/j.plipres.2019.01.003

55. Costa E, Silva J, Mendonça S, Abreu MH, Domingues MR. Lipidomic approaches towards

deciphering glycolipids from microalgae as a reservoir of bioactive lipids. *Mar Drugs*. 2016;14(101):1-27. doi:10.3390/md14050101

56. Christie W. Betaine lipids. The LipidWeb. https://www.lipidmaps.org/resources/lipidweb/index.php?page=lipids/complex/betaine/index.htm . Published 2019. Accessed February 27, 2020.

57. Miazek K, Lebecque S, Hamaidia M, et al. Sphingolipids: promising lipid-class molecules with potential applications for industry. A review. *Biotechnol Agron Soc Environ*. 2016;20. doi:10.25518/1780-4507.13071

58. Yao L, Gerde JA, Lee S, Wang T, Harrata KA. Microalgae lipid characterization. *Agric food Chem*. 2015;63(6):1773-1787. doi:10.1021/jf5050603.

59. Dhargalkar VK, Pereira N. Seaweed: Promising plant of the millennium. *Sci Cult*. 2005.

60. Dembitsky VM, Pechenkina-Shubina EE, Rozentsvet OA. Glycolipids and fatty acids of some seaweeds and marine grasses from the black sea. *Phytochemistry*. 1991;30(7):2279-2283. doi:https://doi.org/10.1016/0031-9422(91)83630-4

61. Chester MA. Nomenclature of glycolipids. *Pure Appl Chem*. 1997;69(12):2475-2487. doi:https://doi.org/10.1351/pac199769122475

62. Plouguerné E, Gama A. P. B, Pereira C. R, Barreto-Bergter E. Glycolipids from seaweeds and their potential biotechnological applications. *Front Cell Infect Microbiol*. 2014;4:174. doi:10.3389/fcimb.2014.00174

63. Zhang J, Li C, Yu G, Guan H. Total synthesis and structure-activity relationship of glycoglycerolipids from marine organisms. *Mar Drugs*. 2014;12(6):3634-3659. doi:10.3390/md12063634

64. Boudière L, Michaud M, Petroutsos D, et al. Glycerolipids in photosynthesis: composition, synthesis and trafficking. *Biochim Biophys Acta*. 2013;1837(4):470-480. doi:10.1016/j.bbabio.2013.09.007

65. Goss R, Wilhelm C. Lipids in algae, lichens and mosses. In: Wada H, Murata N, eds. *Lipids in Photosynthesis: Essential and Regulatory Functions*. Springer Science + Business Media B.V. 2009; 2009:117-135. doi:10.1007/978-90-481-2863-1

66. White DA, Rooks PA, Kimmance S, et al. Modulation of polar lipid profiles in *Chlorella* sp. in response to nutrient limitation. *Metabolites*. 2019;9(39):1-19. doi:10.3390/metabo9030039

67. Wang X, Shen Z, Miao X. Nitrogen and hydrophosphate affects glycolipids composition in microalgae. *Nat Publ Gr*. 2016;6(1). doi:10.1038/srep30145

68. Kumari P, Kumar M, Reddy CRK, Jha B. Nitrate and phosphate regimes induced lipidomic and biochemical changes in intertidal macroalga Ulva lactuca (Ulvophyceae, Chlorophyta). *Plant Cell Physiol*. 2013;55(1):52-63. doi:10.1093/pcp/pct156

69. Plouguerné E, Souza L, Sassaki G, et al. Antiviral sulfoquinovosyldiacylglycerols (SQDGs) from the brazilian brown seaweed *Sargassum vulgare*. *Mar Drugs*. 2013;11(11):4628-4640. doi:10.3390/md11114628

70. Chirasuwan N, Chaiklahan R, Kittakoop P, et al. Anti HSV-1 activity of sulphoquinovosyl diacylglycerol isolated from *Spirulina platensis*. *ScienceAsia*. 2009;35:137-141. doi:10.2306/scienceasia1513-1874.2009.35.137

71. Souza LM De, Sassaki GL, Teresa M, Romanos V. Structural characterization and anti-HSV-1 and HSV-2 activity of glycolipids from the marine algae Osmundaria obtusiloba isolated from southeastern brazilian coast. *Mar Drugs*. 2012;10:918-931. doi:10.3390/md10040918

72. Lee DY, Lin X, Paskaleva EE, et al. Palmitic acid is a novel CD4 fusion inhibitor that blocks HIV entry and infection. *AIDS Res Hum retrovirusses*. 2009;25:1231-1241. doi:10.1089=aid.2009.0019

73. Librán-pérez M, Pereiro P, Figueras A, Novoa B. Antiviral activity of palmitic acid via autophagic flux inhibition in zebrafish (*Danio rerio*). *Fish Shellfish Immunol*. 2019;95:595-605.

doi:10.1016/j.fsi.2019.10.055

74. Abd El Baky HH, El Baz FK, El Baroty GS, Asker MMS, Ibrahim EA. Phospholipids of some marine microalgae: Identification, antivirus, anticancer and antimicrobial bioactivities. *Der Pharma Chem*. 2014;6(6):9-18.

75. Li Y, Lou Y, Mu T, et al. Sphingolipids in marine microalgae: development and application of a mass spectrometric method for global structural characterization of ceramides and glycosylceramides in three major phyla. *Anal Chim Acta*. 2017;986:82-94. doi:10.1016/j.aca.2017.07.039

76. Khotimchenko S V, Kulikova I V, Vas'kovskii VE. Distribution of ceramidephosphoinositol in red seaweeds. *Russ J Mar Biol*. 2000;26(4):286-288. doi:10.1007/BF02759510

77. Merrill A. Chapter 14: Sphingosine and other long-chain bases that alter cell behavior. In: *Current Topics in Membranes*. Vol 40. First Edit. Atlanta: Elsevier Masson SAS; 1994:361-386. doi:10.1016/S0070-2161(08)60988-0

78. Futerman AH. Chapter 10: Sphingolipids. In: *Biochemistry of Lipids, Lipoproteins and Membranes*. Sixth Edit. Elsevier; 2016:297–326. doi:10.1016/B978-0-444-63438-2.00010-9

79. Hussain G, Wang J, Rasul A, et al. Role of cholesterol and sphingolipids in brain development and neurological diseases. *Lipids Health Dis*. 2019;18(26):1-12.

80. Cañavate JP, Armada I, Ríos JL, Hachero-cruzado I. Exploring occurrence and molecular diversity of betaine lipids across taxonomy of marine microalgae. *Phytochemistry*. 2016;124:68-78. doi:10.1016/j.phytochem.2016.02.007

81. Roche S, Leblond J. Betaine lipids in chlorarachniophytes. *Phycol Res*. 2010;58:298-305. doi:10.1111/j.1440-1835.2010.00590.x

82. Siegenthaler P-A, Murata N. Chapter 1: Lipids in photosynthesis - an overview. In: Siegenthaler P-A, Murata N, eds. *Lipids in Photosynthesis: Structure, Function and Genetics*. Illinois: Kluwer Academic Publishers; 2004:1-20.

83. Meng Y, Cao X, Yang M, Liu J, Yao C, Xue S. Glycerolipid remodeling triggered by phosphorous starvation and recovery in *Nannochloropsis oceanica*. *Algal Res*. 2019;39. doi:10.1016/j.algal.2019.101451

84. Srivastava M. Chapter 1: An overview of HPTLC - a modern analytical technique with excellent potential for automation, optimization, hyphenation and multidimensional applications. In: *High-Performance Thin-Layer Chromatography (HPTLC)*. ; 2011:3-24. doi:10.1007/978-3-642-14025-9

85. K. S, Shree B, Lakshmi KS. HPTLC method development and validation: an overview. *J Pharm Sci Res*. 2017;9(5):652-657. doi:10.6227/jfda.2012200408

86. Patel R, Patel M, Batel B. Chapter 3: Experimental aspects and implementation of HPTLC. In: *High-Performance Thin-Layer Chromatography (HPTLC)*. ; 2011:41-54. doi:10.1007/978-3-642-14025-9

87. Ramu B, Chittela KB. High performance thin layer chromatography and its role pharmaceutical industry: review. *Open Sci J Biosci Bioeng*. 2018;5(3):29-34.

88. Rashmin P, Mrunali P, Nitin D, Nidhi D, Bharat P. HPTLC method development and validation: strategy to minimize methodological failures. *J Food Drug Anal*. 2012;20(4):794-804. doi:10.6227/jfda.2012200408

89. Kranjc E, Albreht A, Vovk I, Glavnik V. High performance thin-layer chromatography – mass spectrometry enables reliable analysis of physalins in different plant parts of *Physalis alkekengi* L. *J Chromatogr A*. 2017;1526:137-150. doi:10.1016/j.chroma.2017.09.070

90. Kasote D, Ahmad A, Chen W, Combrinck S, Viljoen A. HPTLC-MS as an efficient hyphenated technique for the rapid identification of antimicrobial compounds from propolis. *Phytochem Lett*. 2014;11:6-11. doi:10.1016/j.phytol.2014.08.017

91. Gupta AP, Gupta S. Chapter 15: HPTLC-MS coupling - new dimension of HPTLC. In: *High-Performance Thin-Layer Chromatography (HPTLC)*. ; 2011:311-333. doi:10.1007/978-3-642-14025-9

92. Coskun O. Separation techniques: chromatography. *Biochemistry*. 2016;3(2):156-160. doi:10.14744/nci.2016.32757

93. CAMAG. *Instructions Manual: Linomat 5*.; 2016.

94. CAMAG. *Instruction Manual: ADC 2*.; 2016.

95. CAMAG. CAMAG® chromatogram immersion device 3. https://www.camag.com/product/camag-chromatogram-immersion-device-3. Accessed December 15, 2019.

96. CAMAG. *Instruction Manual: TLC Scanner 4*.; 2016.

97. Shinde D, Chavan M, Wakte P. Chapter 8: HPTLC in herbal drug quantification. In: *High-Performance Thin-Layer Chromatography (HPTLC)*. ; 2011:117-139. doi:10.1007/978-3-642-14025-9

98. Bridwell H, Dhingra V, Peckman D, Roark J. Perspectives on method validation: importance of adequate method validation. *Qual Assur J*. 2010;13:72-77. doi:10.1002/qaj

99. Thompson M, Ellison S, Wood R. Harmonized guidelines for single-laboratory validation of methods of analysis. *Pure Appl Chem*. 2002;74(5):835-855.

100. Menana M. Implementação e validação do método de quantificação de ácido propiónico por HPLC em produtos de padaria e pastelaria. 2017.

101. Relacre. *Guia RELACRE 13: Validação de Métodos Internos de Ensaio Em Análise Química*. Associação de laboratórios Acreditados de Portugal; 2000.

102. Rathore AS, Lohidasan S, Mahadik KR. Development of validated HPLC and HPTLC methods for simultaneous determination of Levocetirizine Dihydrochloride and Montelukast Sodium in bulk drug and pharmaceutical dosage form. *Pharm Anal Acta*. 2010;1(1). doi:10.4172/2153-2435.1000106

103. Tantawy MA, Hassan NY, Elragehy NA, Abdelkawy M. Simultaneous determination of olanzapine and fluoxetine hydrochloride in capsules by spectrophotometry, TLC-spectrodensitometry and HPLC. *J Adv Res*. 2013;4(2):173-180. doi:10.1016/j.jare.2012.05.004

104. IPAC. *Guia Para a Acreditação de Laboratórios Químicos (OGC002)*.; 2011.

105. Miller JN, Miller JC. *Statistics and Chemometrics for Analytical Chemistry*. Sixth Edit. Edinburgh: Pearson Education Limited; 2010.

106. Martins A. Implementação e validação de métodos analíticos. 2016.

107. Bligh EG, Dyer WJ. A rapid method of total lipid extraction and purification. *Can J Biochem Physiol*. 1959;37(8):911-917. doi:https://doi.org/10.1139/o59-099

108. Folch J, Lees M, Stanley GH. A simple method for the isolation and purification of total lipids from animal tissues. *J Biol Chem*. 1956;226:497-509.

109. Cañavate JP, Armada I, Hachero-Cruzado I. Polar lipids analysis of cultured phytoplankton reveals significant inter-taxa changes, low influence of growth stage, and usefulness in chemotaxonomy. *Microb Ecol*. 2016;73:755-774. doi:10.1007/s00248-016-0893-7

110. Christie W. *Lipid Analysis: Isolation, Separation, Identification and Lipidomic Analysis*. Fourth edi. (Christie W, ed.). Bridgewater, England: The Oil Press; 2003.

111. Dittmer J, Lester R. A simple, specific spray for the detection of phospholipids on thin-layer chromatograms. *J Lipid Res*. 1964;5:126-127.

112. Cohen Z, Vonshak A, Richmond A. Effect of environmental conditions on fatty acid composition of the red alga *Porphyridium cruentum*: correlation to grow rate. *J Phycol*. 1988;24:328-332.

113. Bandarra N, Batista I, Nunes ML, Empis JM, Christie WW. Seasonal Changes in Lipid Composition of Sardine (*Sardina pilchardus*). *J Food Sci*. 1997;62(1):40-42. doi:10.1111/j.1365-2621.1997.tb04364.x

114. CyberLink. General procedures to separate lipid fractions. http://cyberlipid.gerli.com/adsorption-chromatography/simple-procedures/. Accessed May 1, 2020.

115. Iverson SJ, Lang SLC, Cooper MH. Comparison of the Bligh and Dyer and Folch methods for total lipid determination in a broad range of marine tissue. *Lipids*. 2001;36(11):1283-1287. doi:10.1007/s11745-001-0843-0.

116. Gosch B, Magnusson M, Paul N, Nys R. Total lipid and fatty acid composition of seaweeds for the selection of species for oil-based biofuel and bioproducts. *GCB Bioenergy*. 2012;4:919-930. doi:10.1111/j.1757-1707.2012.01175.x

117. Honya M, Kinoshita T, Ishikawa M, Mori H, Nisizawa K. Seasonal variation in the lipid content of cultured *Laminaria japonica*: fatty acids, sterols, b-carotene and tocopherol. *J Appl Phycol*. 1994;6:25-29.

118. Nomura M, Kamogawa H, Susanto E. Seasonal variations of total lipids, fatty acid composition, and fucoxanthin contents of *Sargassum horneri* (Turner) and *Cystoseira hakodatensis* (Yendo) from the northern seashore of Japan. *J Apply Phycol*. 2013;25:1159-1169. doi:10.1007/s10811-012-9934-x

119. Moreno P, Petkov G, Ramazanov Z, Garsia G. Lipids, fatty acids and sterols of *Cystoseira abies-marina*. *Bot Mar*. 1998;41:375-378.

120. Nunes N, Valente S, Ferraz S, Barreto MC, Pinheiro de Carvalho M. Nutraceutical potential of *Asparagopsis taxiformis* (Delile) trevisan extracts and assessment of a downstream purification strategy. *Heliyon*. 2018;4(11). doi:10.1016/j.heliyon.2018.e00957

121. Hajmalek M, Goudarzi M, Ghaffari S, Attar H. Development and validation of a HPTLC method for analysis of Sunitinib malate. *Brazilian J Pharm Sci*. 2016;52(4). doi:10.1590/S1984-82502016000400003

122. Chepurwar SB, Shirkhedkar AA, Bari SB, Fursule RA, Surana SJ. Validated HPTLC Method for simultaneous estimation of levofloxacin hemihydrate and ornidazole in pharmaceutical dosage form. *J Chromatogr Sci*. 2007;45. doi:10.1093/chromsci/45.8.531

123. Masota N, Sempombe J, Tibalinda P, Kaale EA. Development and validation of an HPTLC densitometric method for assay of griseofulvin in tablets. *East Cent African J Pharm Sci*. 2015;18:3-9. doi:10.1016/j.bfopcu.2014.09.002

124. John J, Reghuwanshi A, Aravind UK, Aravindakumar CT. Development and validation of a high-performance thin layer chromatography method for the determination of cholesterol concentration. *J Food Drug Anal*. 2014;23(2):219-224. doi:10.1016/j.jfda.2014.07.006

125. EURL. *Guidance Document on the Estimation of LoD and LoQ for Measurements in the Field of Contaminants in Feed and Food*.; 2016.

126. Attimarad M, Amed KK M, Harsha S. High-performance thin layer chromatography: a powerful analytical technique in pharmaceutical drug discovery. *Pharm Methods*. 2011;2(2):71-75. doi:10.4103/2229-4708.84436

127. Khotimchenko S V., Kulikova I V. Lipids of different parts of the Lamina of Laminaria japonica Aresch. *Bot Mar*. 2000;43:87-91. doi:10.1515/BOT.2000.008

128. Kumari P. Chapter 4: Seaweed lipidomics in the era of 'omics' biology: a contemporary perspective. In: Kumar M, Ralph P, eds. *Systems Biology of Marine Ecosystems*. Gewerbestrasse: Springer International Publishing; 2017:49-97. doi:10.1007/978-3-319-62094-7

129. Kumari P, Kumar M, Reddy C, Jha B. Chapter 3: Algal lipids, fatty acids and sterols. In: Dominguez H, ed. *Functional Ingredients from Algae for Foods and Nutraceuticals*. Woodhead Publishing Limited; 2013:87-133. doi:10.1533/9780857098689

130. Gerasimenko NI, Skriptsova A V, Busarova NG, Moiseenko OP. Effects of the season and growth

stage on the contents of lipids and photosynthetic pigments in brown Alga *Undaria pinnatifida*. *Russ J Plant Physiol*. 2011;58(5):885-891. doi:10.1134/S1021443711050086

131. Gerasimenko NI, Busarova NG, Moiseenko OP. Seasonal changes in the content of lipids, fatty acids, and pigments in brown alga *Costaria costata*. *Russ J Plant Physiol*. 2010;57(2):217-223. doi:10.1134/S102144371002007X

132. Sanina NM, Goncharova SN, Kostetsky EY. Fatty acid composition of individual polar lipid classes from marine macrophytes. *Phytochemistry*. 2004;65(6):721-730. doi:10.1016/j.phytochem.2004.01.013

133. Dembitsky VM, Rozentsvet OA, Pechenkina EE. Glycolipids, phospholipids and fatty acids of brown algae species. *Phytochemistry*. 1990;29(11):3417-3421. doi:10.1016/0031-9422(90)85249-F

134. Jones L, Harwood L. Lipid composition of the brown algae *Fucus vesiculosus* and *Ascophyllum nodosum*. *Phytochemistry*. 1992;31(10):3397-3403. doi:10.1016/0031-9422(92)83693-S

135. Nelson MM, Phleger CF, Nichols PD. Seasonal lipid composition in macroalgae of the Northeastern Pacific Ocean. *Bot Mar*. 2002;45(1):58-65. doi:10.1515/BOT.2002.007

136. Khotimchenko S V, Vaskovsky VE, Titlyanova T V. Fatty Acids of Marine Algae from the Pacific Coast of North California. *Bot Mar*. 2002;45:17-22. doi:10.1515/BOT.2002.003

137. Pereira H, Barreira L, Figueiredo F, et al. Polyunsaturated fatty acids of marine macroalgae: potential for nutritional and pharmaceutical applications. *Mar Drugs*. 2012;10:1920-1935. doi:10.3390/md10091920

138. Frikha F, Kammoun M, Lassaad B, Gargouri Y. Chemical composition and some biological activities of marine algae collected in Tunisia. *Ciencias Mar*. 2011;37(2):113-124. doi:10.7773/cm.v37i2.1712

139. Calder PC. Omega-3 Fatty Acids and Inflammatory Processes. *Nutrients*. 2010;2:355-374. doi:10.3390/nu2030355

140. Tallima H, El R. Arachidonic acid: physiological roles and potential health benefits – a review. *J Adv Res*. 2017;11:33-41. doi:10.1016/j.jare.2017.11.004

141. Ahmed N, Ahmed K. Chemical and different nutritional characteristics of brown seaweed lipids. *Adv Sci Technol Eng Syst*. 2016;1(1):23-25. doi:10.25046/aj010104

142. Bell J, Sargent JR. Arachidonic acid in aquaculture feeds: current status and future opportunities. *Aquaculture*. 2003;218:491-499. doi:10.1016/S0044-8486(02)00370-8

143. Mühlroth A, Li K, Røkke G, et al. Pathways of lipid metabolism in marine algae, co-expression network, bottlenecks and candidate genes for enhanced production of EPA and DHA in species of chromista. *Mar Drugs*. 2013;11:4662-4697. doi:10.3390/md11114662

144. Bieren JE. Eicosanoids in tissue repair. *Immunol Cell Biol*. 2019;97(3):279-280. doi:10.1111/imcb.12226

145. Silva JR, Burger B, Kühl CMC, Candreva T, Anjos MBP, Rodrigues HG. Wound healing and omega-6 fatty acids: from inflammation to repair. *Mediators Inflamm*. 2018;6:1-17. doi:10.1155/2018/2503950

146. Souza EO De, Lowery RP, Wilson JM, et al. Effects of arachidonic acid supplementation on acute anabolic signaling and chronic functional performance and body composition adaptations. *PLoS One*. 2016;11(5):1-20. doi:10.1371/journal.pone.0155153

147. Mitchell CJ, Souza RFD, Figueiredo XVC, et al. Effect of dietary arachidonic acid supplementation on acute muscle adaptive responses to resistance exercise in trained men: a randomized controlled trial. *J Apply Phycol*. 2018;125(35):1080-1091. doi:10.1152/japplphysiol.01100.2017

148. Kawashima H. Intake of arachidonic acid-containing lipids in adult humans: dietary surveys and clinical trials. *Lipids Health Dis*. 2019;18:1-9. doi:10.1186/s12944-019-1039-y

149. Martins D, Rocha F, Castanheira F, et al. Effects of dietary arachidonic acid on cortisol production and gene expression in stress response in Senegalese sole (*Solea senegalensis*) post-larvae. *Fish Physiol Biochem*. 2013;39(5):1223-1238. doi:10.1007/s10695-013-9778-6

150. Herrera M, Mancera JM, Costas B. The use of dietary additives in fish stress mitigation: comparative endocrine and physiological responses. *Front Endocrionology*. 2019;10(447). doi:10.3389/fendo.2019.00447

151. Chee W, Turchini GM, Teoh C, Ng W. Dietary arachidonic acid and the impact on growth performance, health and tissues fatty acids in Malabar red snapper (*Lutjanus malabaricus*) fingerlings. *Aquaculture*. 2019;(November):734757. doi:10.1016/j.aquaculture.2019.734757

152. Galloway AWE, Britton-Simmons KH, Duggins DO, Gabrielson PW, Brett MT. Fatty acid signatures differentiate marine macrophytes at ordinal and family ranks. *Phycol Soc Am*. 2012;47:1-10. doi:10.1111/j.1529-8817.2012.01173.x

153. Li X, Fan X, Han L, Lou Q. Fatty acids of some algae from the Bohai Sea. *Phytochemistry*. 2002;59:157-161. doi:10.1016/s0031-9422(01)00437-x

154. Fonseca I, Guarda I, Mourato M, et al. Undervalued Atlantic brown seaweed species (*Cystoseira abies-marina* and *Zonaria tournefortii*): influence of treatment on their nutritional and bioactive potential and bioaccessibility. *Eur Food Res Technol*. 2020. doi:10.1007/s00217-020-03620-x

155. Chan J, Cheung P. Comparative studies on the effect of three drying methods on the nutritional composition of seaweed *Sargassum hemiphyllum* (Turn.) C. Ag. †. *J Agric Food Chem*. 1997;45:3056-3059. doi:10.1021/jf9701749

156. Hotimchenko S V. Fatty acid composition of algae from habitats with varying amounts of illumination. *Russ J Mar Biol*. 2002;28(3):218-220. doi:10.1023/A:1016861807103

157. Khoeyi Z, Seyfabadi J, Ramezanpour Z. Effect of light intensity and photoperiod on biomass and fatty acid composition of the microalgae, *Chlorella vulgaris*. *Aquacult Int*. 2012;20(6):41-49. doi:10.1007/s10499-011-9440-1

158. Oh S, Lee E, Choe E. Light effects on lipid oxidation, antioxidants, and pigments in dried laver (*Porphyra*) during storage. *Food Sci Biotecnol*. 2014;23(3):701-709. doi:10.1007/s10068-014-0095-3

159. Tao L. Oxidation of polyunsaturated fatty acids and its impact on food quality and human health. *Adv food Technol Nutr Sci*. 2015;1(6):135-142. doi:10.17140/AFTN-SOJ-1-123

160. Magnusson M, Mata L, Nys R De, Paul NA. Biomass, lipid and fatty acid production in large-scale cultures of the marine macroalga *Derbesia tenuissima* (Chlorophyta). *Mar Biotechnol*. 2014;16(4):456-464. doi:10.1007/s10126-014-9564-1

161. Domoto N, Koenen ME, Havenaar R, Mikajiri A, Chu B. The bioaccessibility of eicosapentaenoic acid was higher from phospholipid food products than from mono- and triacylglycerol food products in a dynamic gastrointestinal model. *Food Sci Nutr*. 2013;1(6):409-415. doi:10.1002/fsn3.58

162. Zheng H, Wijaya W, Zhang H, et al. Improving bioaccessibility and bioavailability of carnosic acid using lecithin-based nanoemulsion: complementary in vitro and in vivo studies. *Food Funct*. 2020;(9):7295-8382. doi:10.1039/D0FO01098G

163. Khotimchenko S V. The fatty acid composition of glycolipids of marine macrophytes. *Russ J Mar Biol*. 2003;29(2):126-128. doi:10.1023/A:1023960825983

164. Tsai C, Pan BS. Identification of sulfoglycolipid bioactivities and characteristic fatty acids of marine macroalgae. *J Agric Food Chem*. 2012;60:8404-8410. doi:10.1021/jf302241d

165. Nations U. The 17 goals. Department of Economics and Social Affairs | Sustainable development. https://sdgs.un.org/goals. Published 2020.

7. Annexes

Some results of this work were presented in "JIM: Jornadas Intercalares das Dissertações Anuais dos Mestrados dos Departamentos de Química e de Ciências da Vida 2020" (14th February 2020). Results regarding the brown macroalgae *C. humilis*, were also presented in the online meeting "Lipids in the Ocean 2020" (18th November 2020).

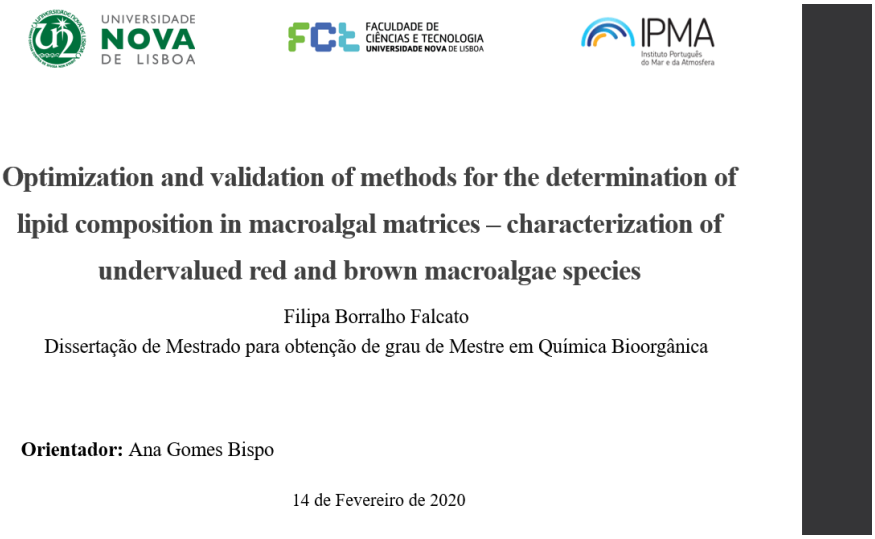
UNIVERSIDADE NOVA DE LISBOA

FACULDADE DE CIÊNCIAS E TECNOLOGIA UNIVERSIDADE NOVA DE LISBOA

IPMA Instituto Português do Mar e da Atmosfera

Optimization and validation of methods for the determination of lipid composition in macroalgal matrices – characterization of undervalued red and brown macroalgae species

Filipa Borralho Falcato

Dissertação de Mestrado para obtenção de grau de Mestre em Química Bioorgânica

Orientador: Ana Gomes Bispo

14 de Fevereiro de 2020

Figure 7.1 Cover of the work presented in "JIM: Jornadas Intercalares das Dissertações Anuais dos Mestrados dos Departamentos de Química e de Ciências da Vida 2020", in Faculty of Sciences and Technology, New University of Lisbon, 14th February 2020.

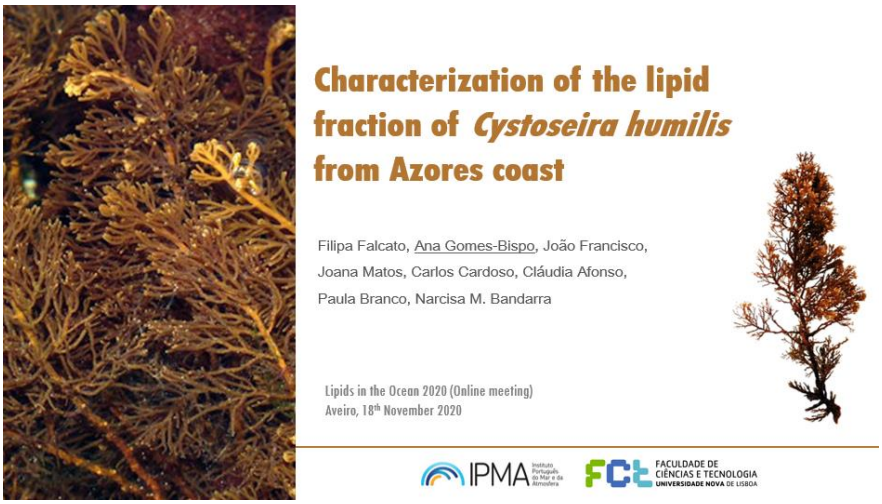

Figure 7.2 Cover of the work presented in the online meeting "Lipids in the Ocean 2020", 18th November 2020.